Response to Editor and Reviewer comments

HESS-2018-580

Title: Multi-model approach to quantify groundwater level prediction uncertainty using an ensemble of global climate models and multiple abstraction scenarios

Authors: Syed M. Touhidul Mustafa*, M. Moudud Hasan, Ajoy Kumar Saha, Rahena Parvin Rannu, Els Van Uytven, Patrick Willems and Marijke Huysmans

We would like to thank the editor and reviewers for reviewing our manuscript very carefully and for their constructive comments. We have considered all the comments and changed the manuscript accordingly. Below is a list of our responses to the editor and reviewer comments (comments in italic, answers in regular font).

Please kindly note that the line numbers in the responses refer to the numbering in the revised manuscript, unless specified.

Editor:

General comments:

You did only partly answered to the reviewers comments. Therefore, provide a revised version of the manuscript with your suggested revisions and improve your answers on the following comments:

RESPONSE: AGREE AND CHANGES MADE

We have clarified our answers to some of the comments as requested and adapted the manuscript and response letter accordingly.

1. - comment 2, rev.1: you have to explain why the calibrated parameters reach the boundary. It makes the calibration questionable.

RESPONSE: AGREE AND CHANGES MADE (lines: 336 - 352).

The following additional explanation about the calibration has been added in the manuscript (lines: 336 - 352).

The optimized value of specific yield varies between 0.17 and 0.35 for different conceptual models. The results are in line with previous finding of specific yield values in the area which indicate that specific yield in the study area varies between 0.08 and 0.32, having higher values in the southern part of the Barind area (Jahan et al., 1994; Mustafa et al., 2018). However, the optimized value of specific yield for some conceptual models are equal to the upper boundary of the pre-defined

parameter range. This could be because of the simplified representation of hydrogeological layers and properties of the system defined in some of the conceptual models. However, even with different conceptual models, the optimized value of specific yield is equal to the upper boundary of the parameter range, indicating that the calibrated values of the specific yield could not reach the real optimum. This could be because of uncertain groundwater abstraction and recharge data in this study area. Mustafa et al. (2018) has proven that groundwater abstraction and groundwater recharge data in space and time in this study area are highly uncertain. They have also reported that input uncertainty (uncertainties arising from groundwater abstraction and recharge) has a significant impact on the specific yield values. However, in this study, uncertainty of the input data has not been considered. Additionally, spatial and seasonal variability of the groundwater abstraction has not been considered in this study. This might be another reason for the high specific yield value. Further improvement of model calibration would require additional and more reliable groundwater abstraction and groundwater recharge data, such as time series of pumping discharge from individual wells and exact locations of all abstraction wells.

Jahan, C.S., Mazumder, Q.H., Ghose, S.K., Asaduzzaman, M., 1994. Specific yield evaluation: Barind area, Bangaladesh. Geol. Soc. India 44(3), 283–290.

Mustafa, S.M.T., Nossent, J., Ghysels, G., Huysmans, M., 2018. Estimation and impact assessment of input and parameter uncertainty in predicting groundwater flow with a fully distributed model. Water Resour. Res. 54(9), 6585-6608.

2. - comment 3, rev.1: you have to explain why the variances are all equal.

RESPONSE: AGREE AND CHANGES MADE

By definition, RMSE values are equal to the square root of the variance. Therefore, there is no added value in using both measures to judge the quality of the models and the variance value and its calculation procedure have been removed from the manuscript.

3. - comment 5, rev. 1: Improve the discussion of the calibration results. Some of the differences are important. Are they located in some specific locations?

RESPONSE: AGREE AND CHANGES MADE (lines: 527 – 541)

We believe that the observations wells with high differences between modelled and observed hydraulic heads are located close to pumping wells about which the information about their

locations and pumping discharge is highly uncertain in this study area. In order to discuss this issue in the manuscript, the relevant section in the original manuscript has been updated with additional information and explanation as follows.

Figure 5 shows the scatter plot for model L2B5. One of the possible causes of the observed differences is the spatial and temporal variation in groundwater abstraction. The zone-wise spatially distributed groundwater abstraction rate was one of the most important input data in this study. In reality, groundwater abstraction varies spatially within those zones. Agricultural and industrial areas abstract more groundwater than wetlands or forest areas. Moreover, groundwater abstraction rate also varies in time following cropping seasons and precipitation patterns. However, an average constant groundwater abstraction rate was assumed for six months (from November to April) in the model. The difference between observed and simulated are high for some observation wells. Those observation wells might be located near to abstraction wells. For observation wells close to groundwater abstraction wells, drawdown by groundwater abstraction could affect observed groundwater heads. This spatial and temporal difference in actual groundwater abstraction and modeled groundwater abstraction causes spatial and temporal variation in simulated and observed groundwater levels. The simplified representation of hydrogeological layers and properties could be also a possible cause of the differences between simulated and observed groundwater levels. For simplification, the aquifer was assumed homogeneous but in reality the aquifer is heterogeneous and this may affect groundwater flow in the aquifer. Also, measurement errors in observation data may influence model performance.

Reviewer #1:

General comments:

The aim of the paper is to make a prediction of a future groundwater level, and to quantify the uncertainty of multiple sources of the models. This is achieved by using multiple conceptual hydrogeological models, climate scenarios and abstraction scenarios. I think the authors conducted a challenging project and present worthwhile results. A relatively simple hydrogeological model is applied which makes that the results have to be judged to that background. The paper has a clear structure and is well written.

Specific comments:

1. Line 273 The magnitude of the river bed conductance is given as 0.18 mˆ2/s (~15500 mˆ2/d). It is unclear what this quantity means. Usually, in MODFLOW the river bed conductance depends on the river length (L) and width (L) within a grid cell, and the (vertical) hydraulic conductivity (L/T) and the

thickness (L) of the river bed. This yields a value with dimension (L^2/T). This is also the dimension of the given conductance, instead of the expected dimension (L/T).

I ask the authors to explain the interpretation of this quantity.

RESPONSE: AGREE AND CHANGES MADE (lines: 273 - 280)

Riverbed conductance is indeed defined as a lumped parameter in MODFLOW defined as:

$$\text{CRIV} = \frac{K_{riv} \times L \times W}{M_{riv}}$$

Where, CRIV= Riverbed hydraulic conductance (L^2T^{-1})

K_{riv} = riverbed sediment hydraulic conductivity (LT^{-1})

L = Length of the river within a grid cell (L)

W = Width of the river within a grid cell (L)

M_{riv} = Thickness of the riverbed within a grid cell (L).

From the equation, it is clear that riverbed hydraulic conductance depends on grid-size, riverbed sediment hydraulic conductivity and thickness of the riverbed. Mehl and Hill (2010) have reported that riverbed conductance depends heavily on grid-size of the model. Hence, direct interpretation on the quantity of riverbed hydraulic conductance is not straightforward.

This additional explanation and motivation were added to the manuscript (lines: 273 - 280).

Mehl, S., & Hill, M. C. (2010). Grid-size dependence of Cauchy boundary conditions used to simulate stream–aquifer interactions. Advances in water resources, 33(4), 430-442.

2. Line 304 The model is calibrated using PEST. The values of the calibrated parameters are given in the supplementary materials in Table SM-2. The calibrated values of the L1 models are 6.00E-3 m/s (518 m/d) and 4.45E-3 m/s (384 m/d) which seem to be unrealistic high values for the described subsurface. The same order of magnitude holds for the second layer of the L2 models, and for the third layer of the L3 models.

Many calibrated parameters are set to the upper boundary of the parameter range. This suggests that the calibrated values could not reach the real optimum, or that conceptual problems in the models prevent a good calibration.

From these observations it may be concluded that the calibration of the hydrogeological model needs more attention. The achieved results, as described in the paper, have to be judged with in relation to the quality of the hydrogeological models.

I ask the authors to add a discussion of the quality of the calibration, and to explain the magnitude of the conductivity values and their validity in the model.

I suggest the authors to add in the discussion an improvement of the calibration in a future study

RESPONSE: AGREE AND CHANGES MADE (lines: 317 – 331; 336 – 352 and 786 – 790)

The optimized horizontal hydraulic conductivity of the one-layered models varies between 4.45 $\times 10^{-03}$ m/s and 6.00 $\times 10^{-03}$ m/s. This high value of horizontal hydraulic conductivity corresponds to well-sorted coarse sand and gravel (Fetter, 2001). We consider these values to be realistic since a major portion of the aquifer consists of coarse sand and coarse sand with gravel. The average horizontal hydraulic conductivity of Bengal basin found by Michael & Voss (2009b) was also high (5 $\times 10^{-04}$ m/s). They also reported that based on the drill-log analysis horizontal hydraulic conductivity of Bengal basin may varies from 6 $\times 10^{-06}$ m/s to 3.00 $\times 10^{-03}$ m/s. The area of the Bengal basin is about 2.8$\times$ 10^5 km^2, but the study area is only a small part of the Bengal basin. Therefore, it is possible that the horizontal hydraulic conductivity is relatively higher in our study area. Bonsor et al. (2017) have also reported in their review report that aquifer materials in the Bengal basin are highly permeable. Mustafa et al. (2018) have also reported that average horizontal hydraulic conductivity of this study area is high and around 2.5 $\times$ 10^{-3} and 4.5 $\times$ 10^{-3} m/s.

Additionally, spatial variability of horizontal hydraulic conductivity has not been considered in this study. We consider an average horizontal conductivity for all individual layers. This might be another reason for high horizontal hydraulic conductivity.

We agree with the reviewer's view that the calibration of the hydrogeological model needs more attention to constrain model parameters. Model calibration using a global optimization method is more reliable than a optimization tool like PEST. However, Mustafa et al. (2018) have also reported in their research paper on uncertainty estimation and impact assessment using global optimization that average horizontal hydraulic conductivity of this study area is high and around 2.5 $\times$ 10^{-3} - 4.5 $\times$ 10^{-3} m/s.

All the details on the magnitude of hydraulic conductivity and model calibration processes have been added to the revised manuscript (lines: 317 – 331).

The following additional explanation about the calibration has been added in the manuscript (lines: 336 - 352).

The optimized value of specific yield varies between 0.17 and 0.35 for different conceptual models. The results are in line with previous finding of specific yield values in the area which indicate that specific yield in the study area varies between 0.08 and 0.32, having higher values in the southern part of the Barind area (Jahan et al., 1994; Mustafa et al., 2018). However, the optimized value of specific yield for some conceptual models are equal to the upper boundary of the pre-defined parameter range. This could be because of the simplified representation of hydrogeological layers and properties of the system defined in some of the conceptual models. However, even with different conceptual models, the optimized value of specific yield is equal to the upper boundary of the parameter range, indicating that the calibrated values of the specific yield could not reach the real optimum. This could be because of uncertain groundwater abstraction and recharge data in this study area. Mustafa et al. (2018) has proven that groundwater abstraction and groundwater recharge data in space and time in this study area are highly uncertain. They have also reported that input uncertainty (uncertainties arising from groundwater abstraction and recharge) has a significant impact on the specific yield values. However, in this study, uncertainty of the input data has not been considered. Additionally, spatial and seasonal variability of the groundwater abstraction has not been considered in this study. This might be another reason for the high specific yield value. Further improvement of model calibration would require additional and more reliable groundwater abstraction and groundwater recharge data, such as time series of pumping discharge from individual wells and exact locations of all abstraction wells.

We have also added to the discussion section that in this study, alternative conceptual models have been calibrated using PEST. However, different calibration methods can result in different calibrated model parameters. Hence, further studies could be conducted using different calibration methods (e.g. global parameters optimization methods). We also advice that more field data would be collected, such as reliable groundwater abstraction data, river flow information, spatially distributed horizontal hydraulic conductivity and detailed information about the boundary conditions. (lines: 786 – 790).

Bonsor, H.C., MacDonald, A.M., Ahmed, K.M., Burgess, W.G., Basharat, M., Calow, R.C., et al., 2017. Hydrogeological typologies of the Indo-Gangetic basin alluvial aquifer, South AsiaTypologies. Hydrogeol. J. 1–30.

Fetter, C.W., 2001. Applied Hydrogeology. 4th Edition, Prentice Hall, Upper Saddle River, 2, 8.

Jahan, C.S., Mazumder, Q.H., Ghose, S.K., Asaduzzaman, M., 1994. Specific yield evaluation: Barind area, Bangaladesh. Geol. Soc. India 44(3), 283–290.

Michael, H.A., Voss, C.I., 2009b. Controls on groundwater flow in the Bengal Basin of India and Bangladesh: regional modeling analysis. Hydrogeol. J. 17, 1561.

Mustafa, S.M.T., Nossent, J., Ghysels, G., Huysmans, M., 2018. Estimation and impact assessment of input and parameter uncertainty in predicting groundwater flow with a fully distributed model. Water Resour. Res. 54(9), 6585-6608.

3. Line 480 The RMSE and the variance are both used to test the goodness of fit of the models. In table SM-5 and SM-6, however, all RMSE values are exactly equal to the square root of the variance. The description of the variance in line 319 also seems to be the same as the calculation of the RMSE. This suggests that there is no added value to use both measures to judge the quality of the models. Are the authors convinced about the correctness of the implementation of these measures? Or are the calculations of both measures inherently equal?

Please make clear what the value of the variance is or, in the case of equality of both measures, I would suggest to remove the presentation of one of the measures (RMSE or variance) from the results.

RESPONSE: AGREE AND CHANGES MADE

By definition, RMSE values are equal to the square root of the variance. Therefore, there is no added value in using both measures to judge the quality of the models and the variance value and its calculation procedure have been removed from the manuscript.

4. Another presented performance measure is the PBIAS in Eq. 2. This equation is applied to the observed and calculated groundwater levels. Since groundwater levels are measured against an arbitrary reference level I think the PBIAS is not a suitable measure to apply on these values. The numerator of the formula of PBIAS is not affected by the choice of the reference level but the denominator is. The PBIAS measure seems more suitable for quantities without an arbitrary reference level, like fluxes.

I ask the authors to make clear why PBIAS is a good performance indicator in the current study and why it can be used, or to replace it by another indicator or, if they agree with my objections, to remove it from the article.

RESPONSE: AGREE AND CHANGES MADE

PBIAS and its calculation procedure have been removed from the manuscript.

5. *Line 496 The authors describe the cause of the outliers in Fig. 5. It is not explicitly mentioned which observations the authors call the outliers, but it seems to be the observations beyond the 95% interval. Obviously, about 5% of the observations will lie beyond the 95% interval. The presented graph does not have extreme outliers, relatively to the total data cloud. More important is to what extent a difference between observed and calculated values is accepted in this study.*

I ask the authors to make clear what they consider the acceptable difference between observed and calculated values, or which acceptable interval.

RESPONSE: AGREE AND CHANGES MADE (lines: 527 – 541)

There are indeed no extreme outliers. To avoid confusion, the relevant sentences have been updated by removing the word “outliers”.

We believe that the observations wells with high differences between modelled and observed hydraulic heads are located close to pumping wells about which the information about their locations and pumping discharge is highly uncertain in this study area. In order to discuss this issue in the manuscript, the relevant section in the original manuscript has been updated with additional information and explanation as follows.

Figure 5 shows the scatter plot for model L2B5. One of the possible causes of the observed differences is the spatial and temporal variation in groundwater abstraction. The zone-wise spatially distributed groundwater abstraction rate was one of the most important input data in this study. In reality, groundwater abstraction varies spatially within those zones. Agricultural and industrial areas abstract more groundwater than wetlands or forest areas. Moreover, groundwater abstraction rate also varies in time following cropping seasons and precipitation patterns. However, an average constant groundwater abstraction rate was assumed for six months (from November to April) in the model. The difference between observed and simulated are high for some observation wells. Those observation wells might be located near to abstraction wells. For observation wells close to groundwater abstraction wells, drawdown by groundwater abstraction could affect observed groundwater heads. This spatial and temporal difference in actual groundwater abstraction and modeled groundwater abstraction causes spatial and temporal variation in simulated and observed

groundwater levels. The simplified representation of hydrogeological layers and properties could be also a possible cause of the differences between simulated and observed groundwater levels. For simplification, the aquifer was assumed homogeneous but in reality the aquifer is heterogeneous and this may affect groundwater flow in the aquifer. Also, measurement errors in observation data may influence model performance.

6. Line 562 In Fig. 7c the temperature changes calculated in the different scenarios are presented. Herein, the Tmax is lower (instead of higher) depicted than the Tmean and Tmin, which is confusing.

Please explain what these values do represent?

RESPONSE: AGREE AND CHANGES MADE (lines: 579 – 580; 595 – 597)

Figure 7 shows the changes in monthly climatic parameters between the control and scenario period ranging between 1961-1990 and 2021-2050, respectively. Figure 7c shows the absolute changes in monthly minimum, mean and maximum daily temperature between the control and scenario period.

Here, the figures show that the changes in Tmax are lower compared to the changes of Tmean and Tmin.

This section has been updated with this additional clarification to avoid confusion.

7. Line 548 and Line 575 In these lines the period 'dry season' is mentioned. It would help the reader to repeat here which months are considered the dry season.

RESPONSE: AGREE AND CHANGES MADE (lines: 582 and 609)

Months considered for the dry season have been added.

Technical corrections:

8. Line 65: first occurrence of CHMs should be singular

RESPONSE: AGREE AND CHANGES MADE (line: 65)

The additional "S" has been removed from "CHMs".

9. Line 74 increasing -> increasingly

RESPONSE: AGREE AND CHANGES MADE (line: 74)

The word increasing has been replaced by increasingly.

10. Lines 86 abbreviation GHS is explained, Line 87 GHG is used

RESPONSE: AGREE AND CHANGES MADE (line: 87)

Line 87 of the original manuscript has been updated with GHS instead of GHG.

11. The words 'groundwater level' is often written as singular, where it should be plural.

RESPONSE: AGREE AND CHANGES MADE

This has been corrected.

12. I would suggest to add in long sentences commas (",") for readability.

RESPONSE: AGREE AND CHANGES MADE

Commas (",") have been added to the long sentences.

Reviewer # 2

General comments:

This paper deals with uncertainties in groundwater level predictions due to greenhouse gas scenarios, climate models, conceptual hydrogeological models (CHMs) and groundwater abstraction scenarios. To achieve this aim, ensemble of alternative CHMs, recharge and abstraction scenarios were used. The study confirms Bayesian Model Averaging (BMA) is the most suitable technique designed both to develop multi-model ensemble approach and to help account for the uncertainty inherent in the model selection process. The topic of the note lies within the aims and scope of Hydrology and Earth System Sciences and deals with a topic of considerable interest.

Multi-model approaches can be profitably associated with sensitivity analysis in order to answer the following questions: for a given set of measurements, which conceptual picture of the physical processes, as embodied in a mathematical model or models, is most appropriate? What are the most

valuable space-time locations for measurements, depending on the model selected? How is model parameter uncertainty propagated to model output, and how does this propagation affect model calibration? Recent examples of methods to combine sensitivity-based calibration and model selection have been presented in literature right in the context of groundwater modelling. I suggest to the authors to deepen this topic since, at this stage, the paper does not introduce significant scientific advances respect to the state of art. It's true that typically parametric uncertainty dominates in literature with respect to the uncertainty related to models and scenarios. Nevertheless, this is not enough to make the paper self contained. This is a general evaluation on the study that brought me to the decision that the work still needs major revisions to make it acceptable for publication.

RESPONSE: AGREE AND CHANGES MADE: ADDITIONAL EXPLANATION IN THE TEXT (lines: 791 – 796)

We agree with the reviewer that multi-model approaches are associated with sensitivity analysis in order to answer the following questions: for a given set of measurements, which conceptual picture of the physical processes, as embodied in a mathematical model or models, is most appropriate? What are the most valuable space-time locations for measurements, depending on the model selected? How is model parameter uncertainty propagated to model output, and how does this propagation affect model calibration?

However, the main objective of this study was not to identify the optimum parameters set or the best conceptual model structure. Our main objective was to evaluate the combined effect of conceptual hydro(geo)logical models (CHMs) structure, climate change and groundwater abstraction scenarios on future groundwater level prediction uncertainty. That is why we have incorporated all possible alternatives based on the available field data. Additionally, a separate study on the effect of input and parameter uncertainty has been published in Water Resources Research (Mustafa et al., 2018).

In order to highlight the important of sensitivity analysis, the following sentences have been added to the revised manuscript: "Keeping in mind that the complexity of hydrogeological models is increasing, further studies should be conducted on global sensitivity analysis (SA) to (i) identify the influential and non-influential parameters on the model prediction and (ii) better understand the importance of the different components of the complex model structure. Identification of influential parameters will play an important role in model parameterization and in reducing uncertainty due to overparameterization. The identification of non-influential parameters using SA will be a very important step in simplifying model structure".

Mustafa, S. M. T., Nossent, J., Ghysels, G., & Huysmans, M. (2018). Estimation and impact assessment of input and parameter uncertainty in predicting groundwater flow with a fully distributed model. Water Resources Research, 54(9), 6585-6608.

Specific suggestions to improve the quality of the paper are listed below:

1) I suggest to add a schematic representation of the system investigated for the sake of clarity. This will help identifying the calibration parameters in one/two/three-layered models respectively.

RESPONSE: AGREE AND CHANGES MADE (lines: supplementary materials: Table SM-1)

A schematic representation of the system with all details of the calibration parameters used in the one/two/three-layered models, including the number of parameters, has been added in the supplementary materials (Table SM-1).

2) With the goal of facilitating the understanding of the study, it may be worthwhile to insert the equations used in the analysis and not just references.

RESPONSE: AGREE AND CHANGES MADE: ADDITIONAL EXPLANATION ADDED TO THE TEXT

All the relevant equations are given in the manuscript (Equations: 1-15).

3) Please reword paragraphs 2.7 "Future groundwater recharge scenario" providing more details about model adopted and 2.10 "Data analysis" explaining more clearly the procedure followed.

RESPONSE: AGREE AND CHANGES MADE (lines: 421 – 422 and 490)

All the details about the model adopted for this study are explained in section 2.6 of the original manuscript. However, for the sake of clarity, the following sentence has been added in the section 2.7. "Details about the considered climate model runs for this study are explained in section 2.6 and they are listed in the supplementary materials (Table SM-7)".

Section 2.10 has been updated by adding the following sentence: "Details about the procedure followed for data analysis is explained in sections 2.4 to 2.9".

4) Improve the quality/size of the figures to highlight the results of the analysis

RESPONSE: AGREE AND CHANGES MADE

The quality of the figures (Figure 1, 2, 4, 5, 7, 8, 10, and 13) has been improved.

Minor points:

5) Check line 65, "CHMs", remove "s".

RESPONSE: AGREE AND CHANGES MADE (line: 65)

The additional "S" has been removed from "CHMs".

6) Check line 192, in "step" a "s" is missing.

RESPONSE: AGREE AND CHANGES MADE (line: 193)

The sentence has been updated by adding an additional "s".

7) Check line 424, reference is missing.

RESPONSE: AGREE AND CHANGES MADE (line: 460)

A reference has been added.

8) Check Line 480, reference is missing.

RESPONSE: AGREE AND CHANGES MADE (line: 515)

A reference has been added.

Multi-model approach to quantify groundwater level prediction uncertainty using an ensemble of global climate models and multiple abstraction scenarios

Syed M. Touhidul Mustafa [1,*], M. Moudud Hasan[1], Ajoy Kumar Saha[1], Rahena Parvin Rannu[1], Els Van Uytven[2], Patrick Willems [1,2] and Marijke Huysmans [1]

[1]Department of Hydrology and Hydraulic Engineering, Vrije Universiteit Brussel (VUB), Pleinlaan 2, 1050 Brussels, Belgium

[2]Department of Civil Engineering – Hydraulics Section, KU Leuven, Kasteelpark 40 box 2448, 3001 Leuven, Belgium

* Correspondence to: Syed Md Touhidul Mustafa (syed.mustafa@vub.be)

Abstract

Worldwide, groundwater resources are under a constant threat of overexploitation and pollution due to anthropogenic and climatic pressures. For sustainable management and policy making a reliable prediction of groundwater levels for different future scenarios is necessary. Uncertainties are present in these groundwater level predictions and originate from greenhouse gas scenarios, climate models, conceptual hydro(geo)logical models (CHMs) and groundwater abstraction scenarios. The aim of this study is to quantify the individual uncertainty contributions using an ensemble of 2 greenhouse gas scenarios (representative concentration pathway 4.5 and 8.5), 22 global climate models, 15 alternative CHMs and 5 groundwater abstraction scenarios. This multi-model ensemble approach was applied to a drought prone study area in Bangladesh. Findings of this study, firstly, point at the strong dependence of the groundwater levels on the CHMs considered. All groundwater abstraction scenarios showed a significant decrease in groundwater levels. If the current groundwater abstraction trend continues, the groundwater level is predicted to decline about 5 to 6 times faster for the future period 2026-2047 compared to the baseline period (1985–2006). Even with a 30% lower groundwater abstraction rate, the mean monthly groundwater level would decrease by up to 14 m in the southwestern part of the study area. The groundwater abstraction in the northwestern part of Bangladesh has to reduce by 60% of the current abstraction to ensure sustainable use of groundwater. Finally, the difference in abstraction scenarios was identified as the dominant uncertainty source. CHM uncertainty contributed about 23% of total uncertainty. The alternative CHM uncertainty contribution is higher than the recharge scenario uncertainty contribution, including the greenhouse gas scenario and climate model uncertainty contributions. It is recommended that future groundwater level prediction studies should use multi-model and multiple climate and abstraction scenarios.

Keywords

Multi-model ensemble approach; Groundwater modelling; Conceptual models; Climate change; Abstraction scenarios; Uncertainty.

1. Introduction

Groundwater is one of the major sources of high-quality fresh water across the world and one of the most important but scarce natural resources in many arid and semi-arid regions. However, these resources are under a constant threat of overexploitation and pollution all over the world due to anthropogenic and climatic pressure. Globally, groundwater provides 45 – 70 % of irrigation water (Döll et al., 2012; Shamsudduha et al., 2011; Taylor et al., 2013; Wada et al., 2014, 2013; Wisser et al., 2008) and the use of groundwater is continuously increasing. Overexploitation of groundwater for irrigation is worldwide one of the main causes of groundwater level depletion (Mustafa et al., 2017a; Rodell et al., 2009; Scanlon et al., 2012; Wada et al., 2014). Climate change will probably also have an impact on the future availability of the groundwater resources (Brouyère et al., 2004; Chen et al., 2004; Goderniaux et al., 2011, 2009; Scibek et al., 2007; Taylor et al., 2013; van Roosmalen et al., 2009; Woldeamlak et al., 2007).

Food security of Bangladesh is highly dependent on sustainable use of groundwater for irrigation. However, in the northwestern part of Bangladesh, these resources are under a constant threat of overexploitation due to anthropogenic pressure. Mustafa et al. (2017a) report that overexploitation of groundwater for irrigation is the main cause of groundwater level decline in the northwestern part of Bangladesh. In this context, the government of Bangladesh has plans to use more surface water instead of groundwater. However, the amount of groundwater that can be sustainably used for irrigation is still unknown. Also, the probable impact of shifting to more surface water use instead of groundwater is also unknown. Hence, research is needed to quantify the amount of groundwater that can be abstract sustainably for irrigated agriculture in the northwestern part of Bangladesh.

Accurate predictions of groundwater systems, as well as sustainable water management practices, are essential for policy making. Transient numerical groundwater flow models are used to understand and forecast groundwater flow systems under anthropogenic and climatic influences. They provide primary information for decision-making and risk analysis. However, the reliability of groundwater model predictions is strongly influenced by uncertainties resulting from the model parameters, input data, and the CHMs structure (Refsgaard et al., 2006). Also, formulation of unknown future conditions, such as climatic change scenarios and groundwater abstraction strategies, increases the uncertainty in groundwater model predictions.

It is important to assess the different sources of uncertainty to ensure accurate prediction and reliable decision support in sustainable water resources management. The conventional treatment of uncertainty in groundwater modelling focuses on parameter uncertainty. Uncertainties due to model structure and due to scenario change are often neglected (Gaganis and Smith, 2006; Rojas et al., 2010). However, many researchers have recently acknowledged that the uncertainty arising from the CHMs structure has a significant effect on model prediction (Neuman, 2003; Refsgaard et al., 2006). The incomplete and biased representation of the processes and the complex structure of a geological system often result in uncertainty in model prediction (Refsgaard et al., 2006; Rojas et al., 2008). Højberg & Refsgaard (2005) presented a case of a multi-aquifer system in Denmark by building three different CHMs using three alternative geological assumptions. They found that CHMs structure uncertainty dominated over parameter uncertainty when the models were used for extrapolation. Many studies have recently suggested that uncertainty derived from the definition of alternative CHMs is one of the major sources of total uncertainty, and the parameter uncertainty does not cover the entire uncertainty range (Bredehoeft, 2005; Neuman, 2003; Refsgaard et al., 2006; Rojas et al., 2008; Troldborg et al., 2007). Therefore, neglecting the CHM uncertainty may result in unreliable prediction and underestimate the total predictive uncertainty.

Studies using a single CHM~~s~~ may fail to adequately sample the relevant space of plausible CHMs. Single model techniques are unable to account for errors in model output resulting from the structural deficiencies of the specific model. Rojas et al. (2010) noted that a CHM is assumed to be correct when the model is calibrated and validated successfully following an appropriate method as described by Hassan (2004a, 2004b). However, a well-calibrated model does not always accurately predict the behaviour of the dynamic system (Van Straten and Keesman, 1991). Bredehoeft (2005) presented different examples where data collection and unforeseen elements challenged well-established CHMs. Choosing a single model out of equally important alternative models may contribute to either type I (reject true model) or type II (fail to reject false model) model errors (Li and Tsai, 2009; Neuman, 2003).

Although the concept of using alternative CHMs is increasingly applied among surface water modellers, in groundwater modelling the use of multi-model methods are limited. Recently, some studies have used multi-model methods in groundwater modelling to quantify the CHM uncertainty (Li and Tsai, 2009; Rojas et al., 2010). However, conceptual model uncertainty arising from the simplified representation of the hydro(geo)logic processes, geological stratification and/or boundary conditions has received less attention (Refsgaard et al., 2006; Rojas et al., 2010). Rojas et al. (2010), investigated uncertainty related to alternative CHM structures and

recharge scenarios in groundwater modelling. However, the uncertainty arising from other sources such as General Circulation Models (GCMs), Regional Circulation Models (RCMs), downscaling methods and abstraction scenarios in groundwater flow modelling still needs to be included in such approaches.

Climate change may significantly impact groundwater recharge. Recharge is one of the major input data in groundwater levels simulation. The future groundwater recharge is unknown, so it should be estimated based on different future climate scenarios. The GCMs project different climate scenarios based on the greenhouse gas emission scenarios (GHSs). The Special Report on the Emission Scenario-SRES (Nakicenovic et al., 2000) has reported different GHS~~G~~ emission scenarios. Besides, there are many GCMs to predict climate scenarios, and different GCMs use a different representation of the climate system (Flato et al., 2013; Gosling et al., 2011; Teklesadik et al., 2017). That means that different GCMs develop different climate projections for a single GHG emission scenario. Therefore, uncertainties arise in climate projections from GCMs and GHG emission scenarios. Another important source of uncertainties in climate projection is the internal variability of the climate system, i.e., the natural variability of the weather (Deser et al., 2012). Future climate change uncertainty arises from three main sources: external forcing, climate models response and internal variability (Hawkins and Sutton, 2009; Tebaldi and Knutti, 2007). Using an ensemble of climate scenarios has become common practice in analysis of climate change impact in the field of hydrology. Uncertainty analysis of groundwater simulations related to climate change has received relatively limited attention (Goderniaux et al., 2009; Taylor et al., 2013). Holman et al. (2012) recommended that climate scenarios from multiple GCMs or RCMs should be used to predict the impact of climate change on groundwater. Recently, several researchers have studied the impact of climate change on the groundwater system incorporating uncertainty from the input of different GCMs or RCMs scenarios and different greenhouse gas emission scenarios (Ali et al., 2012; Dams et al., 2012; Jackson et al., 2011; Neukum and Azzam, 2012; Stoll et al., 2011; Sulis et al., 2012). The uncertainty analysis is, however, usually limited to the climatic part. Very recently, Goderniaux et al. (2015) included uncertainty related to model calibration in predicting groundwater flow along with uncertainty from the GCMs and RCMs and downscaling methods. However, the uncertainty arising from other sources, such as the model conceptualization and abstraction scenarios, is not evaluated.

Groundwater levels are often heavily influenced by the groundwater abstraction rate. For example, in the Indian subcontinent, groundwater abstraction has increased from 10-20 km^3/year to approximately 260 km^3/year during the last 50 years (Shamsudduha et al., 2011). In the northwestern part of Bangladesh, about 97% of the total groundwater abstraction is used for irrigated agriculture (Mustafa et al., 2017a; Shahid, 2009). Shahid (2011)

found an increasing trend in irrigation application rate in Boro rice, the major irrigated crop in the area. Details on current groundwater abstraction, trends in the abstraction and irrigated area can be found in Mustafa et al. (2017a). This increasing trend is ascribed to climate change. In contrast, improvement in agricultural water use efficiency can reduce the water use in irrigated agriculture. Therefore, multiple abstraction scenarios should be used to predict a reliable uncertainty band.

Existing literature on future groundwater level prediction uncertainty quantification has focused on hydrological model calibration and climate model uncertainty considering one single CHM and parameter uncertainty. As far as the authors are aware, little research has been done so far to quantify future groundwater level prediction uncertainty considering the uncertainty arising from the CHM structure, climate change and groundwater abstraction scenarios. This is the first attempt to evaluate the combined effect of CHM structure, the climate change and groundwater abstraction scenarios on future groundwater level prediction uncertainty.

The general objective of this study is to quantify groundwater level prediction uncertainty in climate change impact studies using a multi model ensemble, i.e. an ensemble of representative concentration pathways, global climate models, multiple alternative CHMs and abstraction scenarios to provide probabilistic and informative predictions of groundwater levels. The specific objectives to achieve the general goal of this study are to: (i) quantify the groundwater level prediction uncertainties arising from the definition of alternative CHMs; (ii) analyse the effect of climate change on the groundwater levels using ensemble global climate models and estimate the uncertainty linked to climate scenarios; (iii) analyse the effect of groundwater abstraction scenarios on the future groundwater levels; (iv) quantify the amount of water that can be abstracted sustainably for irrigated agriculture in the northwestern part of Bangladesh (v) evaluate the combined effect of CHMs structure, the climate change and groundwater abstraction scenarios on future groundwater level prediction uncertainty; and (vi) compare the uncertainty arising from the alternative CHMs, climate scenarios and abstraction scenarios.

2. Methodology

2.1 Study area

The study area is located in the northwestern part of Bangladesh (Figure 1a). The study area is a subtropical region with two distinct seasons: the dry winter season (November to April) and the rainy monsoon season (May to October). The average annual precipitation amount varies between 1400 and 1550 mm but is not uniformly distributed over the year (Supplementary materials: Figure SM-2). Almost 83% of the total annual amount occurs in the monsoon season. The average temperature varies between 25–35 °C for March to June, and 9–15

°C for November to February. Groundwater depth in the study area is continuously increasing (Supplementary materials: Figure SM-3). The study area consists of six northwestern districts (Rajshahi, Naogaon, C'Nawabganj, Joypurhat, Bogra and Nator) and cover about 7112 km^2. In comparison to other districts of Bangladesh, these districts are more affected by drought (Shahid and Behrawan, 2008). The study area is situated between latitude 24°19′′0′′ N to 25°12′0′′ N and longitude 88°6′36′′ E to 89°31′12′′ E. The surface elevation in the study area varies from 11 m to 40 m (Supplementary materials: Figure SM-1). There is a mild gradient towards the southeast corner and this corner is close to a large wet-land.

The aquifer in the study area is comprised of several layers such as clay, loamy clay, fine sand, medium sand, coarse sand and gravel with a dominance of medium to coarse sand (Figure 1c). The thickness of each stratigraphic unit moreover varies spatially. The top layer consists of clay, clayey loam and fine sand with an average thickness of 18 m. It is underlain by a 20 m thick medium sand layer. Below the medium sand layer, a 35 m thick layer of coarse sand and coarse sand with gravel is present. The upper aquifer is unconfined or semi-confined with a thickness ranging from 10 m to 40 m (Asad-uz-Zaman and Rushton, 2006; Faisal et al., 2005; Jahani and Ahmed, 1997; Michael and Voss, 2009a; Rahman and Shahid, 2004). The area is dominated by agriculture and almost 80 % is crop land. Irrigated agriculture plays an important role in the food production and security of Bangladesh, home to over 150 million people. In the northwestern part of Bangladesh irrigated agriculture is the major user of groundwater and accounts for 97 % of total groundwater abstraction (Shahid, 2009). Overexploitation of groundwater for irrigation, particularly during the dry season, causes groundwater-level decline in areas where abstraction is high and surface geology inhibits direct recharge to the underlying shallow aquifer (Mustafa et al., 2017a).

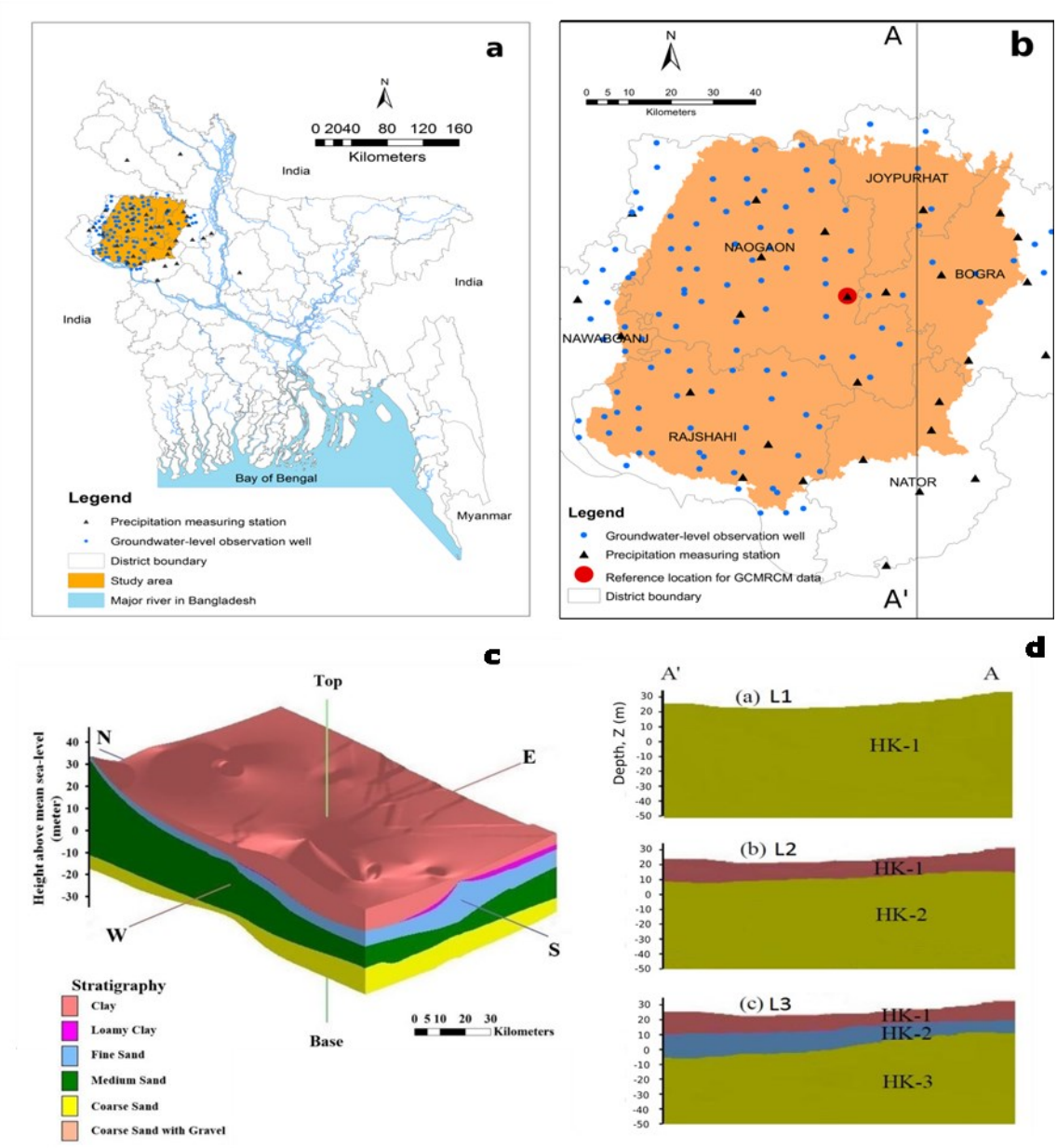
a
N
0 2040 80 120 160
Kilometers
India
India
India
Bay of Bengal
Myanmar
Legend
Precipitation measuring station
Groundwater-level observation well
District boundary
Study area
Major river in Bangladesh
b
N
A
A'
0 5 10 20 30 40
Kilometers
JOYPURHAT
NAOGAON
BOGRA
NAWABGANJ
RAJSHAHI
NATOR
Legend
Groundwater-level observation well
Precipitation measuring station
Reference location for GCMRCM data
District boundary
c
Top
Base
N
E
W
S
Height above mean sea-level (meter)
40 30 20 10 0 -10 -20 -30
0 5 10 20 30
Kilometers
Stratigraphy
Clay
Loamy Clay
Fine Sand
Medium Sand
Coarse Sand
Coarse Sand with Gravel
d
A'
A
Depth, Z (m)
30 20 10 0 -10 -20 -30 -40 -50
(a) L1
HK-1
(b) L2
HK-1
HK-2
(c) L3
HK-1
HK-2
HK-3

159

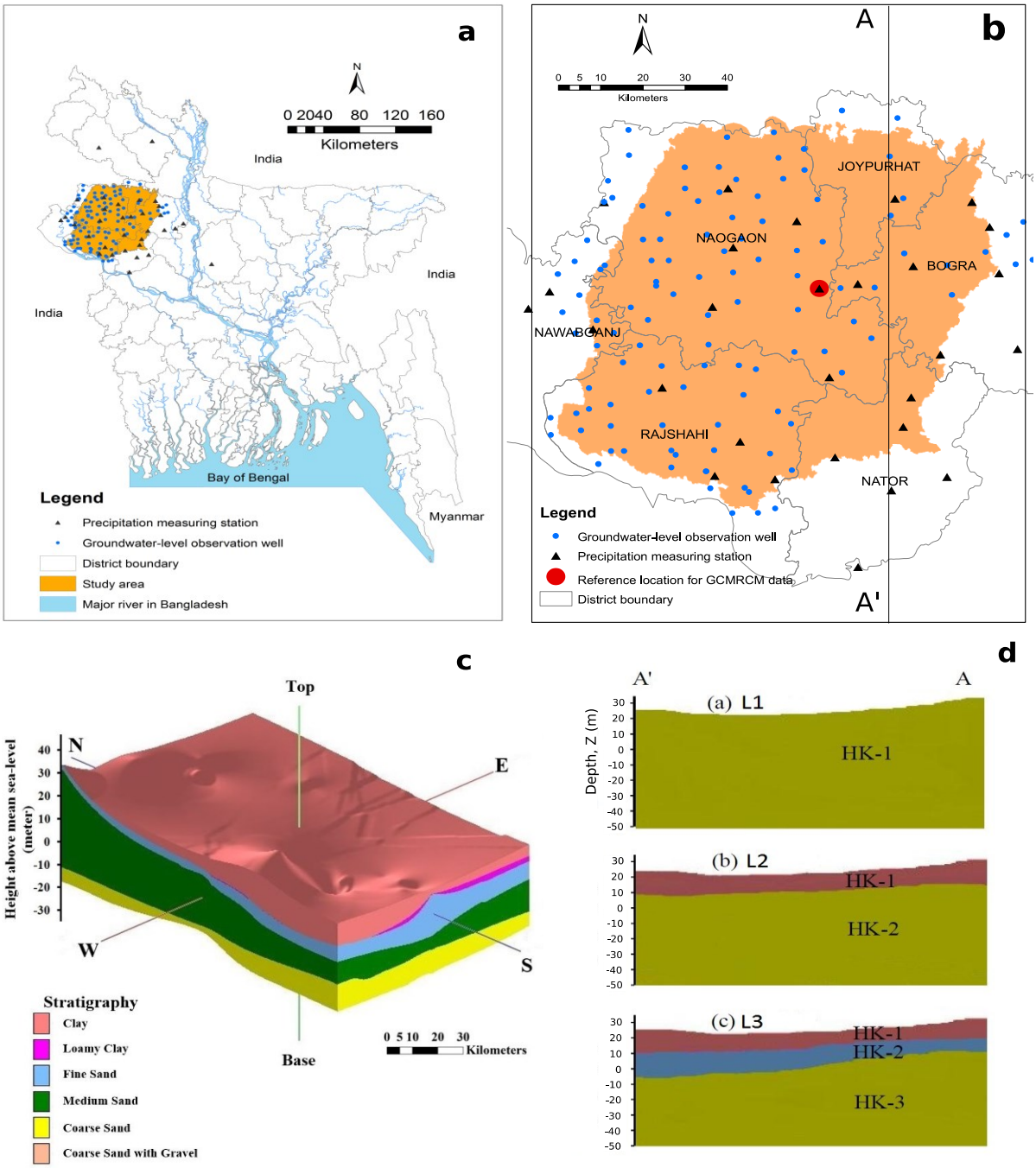

Figure 1: Description of the study area: (a) Location of the study area in the northwestern part of Bangladesh; (b) study area with precipitation measurement stations (triangles) and groundwater observation wells (circles); (c) stratigraphy of the study area; (d) cross-sectional (A-A') view of different models: (a) one-layered model (L1), (b) two-layered model (L2), (c) three-layered model (L3).

2.2 Data

Thirty-two years (1979–2011) of weekly groundwater level and daily precipitation data of the Bangladesh Water Development Board (BWDB) and Bangladesh Meteorological Department (BMD) were collected from the

168 Water Resources Planning Organization (WARPO), Bangladesh, for respectively 140 and 30 sites in the study
169 area. Available river discharge data of the BWDB for the existing small rivers within the study area were also
170 collected from WARPO. Daily minimum and maximum temperature, wind speed and other climatic data were
171 collected from the BMD for all the available stations in the country. Reference evapotranspiration (ET_0),
172 considered as potential evapotranspiration in this study, was calculated using the FAO Penman-Monteith
173 equation from the observed climatic data (Allen et al., 1998; Mustafa et al., 2017a).

174 The monthly observed groundwater head data of 50 observation wells were used for model calibration and
175 validation and are plotted in a box-plot (Supplementary materials: Figure SM-2). The groundwater levels vary
176 between 3 to 22 m above mean sea level (amsl) and display a clear seasonal variation. The groundwater level is
177 relatively low in April and high in October.

178 The hydraulic properties of the aquifers were selected based on observed data and previous reports on the
179 geology and lithology of the study area (Michael and Voss, 2009a, 2009b). Topography and borehole data were
180 collected from Barind Multipurpose Development Authority (BMDA), Bangladesh. The log data from twenty-
181 three boreholes within the study area were collected from BMDA.

182 The climate model data is available through the website of the Earth System Grid Federation
183 (https://esgf.llnl.gov).

184 **2.3 MODFLOW model**

185 Processing MODFLOW or PMWIN (Chiang and Kinzelbach, 1998) is a physically-based, fully-distributed, grid
186 based, integrated simulation system for modelling groundwater flow and pollution. PMWIN was designed as a
187 pre- and postprocessor for the groundwater flow model MODFLOW (Harbaugh and McDonald, 1996;
188 McDonald and Harbaugh, 1988) to bring various codes together in a simulation system. The MODFLOW model
189 is a physically-based, fully-distributed three-dimensional finite-difference numerical flow model developed by
190 the U.S. Geological Survey (USGS). MODFLOW solves the three-dimensional partial-differential groundwater
191 flow equation for porous media using a finite-difference method.

192 **2.4 Multi-step multi-model methodology**

193 A four-steps methodology was used to achieve the objectives of the study (Figure 2). In the first step, the climate
194 model data for precipitation, minimum, mean and maximum temperature and ET_0 were extracted and
195 downscaled as explained in section 2.6. In the second step, monthly groundwater recharge was simulated using a
196 spatially distributed water balance model (WetSpass) (Abdollahi et al., 2017; Batelaan and De Smedt, 2001) for

197 the baseline period and for different scenarios as explained in sections 2.5.2 and 2.7. In the third step, 15
198 alternative conceptual hydrogeological models were constructed using different geological interpretations and
199 boundary conditions. All alternative CHMs were calibrated using observed groundwater level data. The
200 performance of each model was evaluated based on different performance evaluation coefficients and
201 information criterion statistics. The Bayesian model averaging (BMA) method was applied to obtain an average
202 prediction from the alternative models. Also, the performance of alternative models was evaluated based on the
203 maximum likelihood BMA weight of each model. The better performing models among the alternative models
204 were used to project groundwater levels under different climatic and abstraction scenarios. The averaged
205 projection and its uncertainty were estimated using BMA of the ensemble of alternative CHMs. In the final step,
206 climate change impact was assessed. The details of the different materials and methods of each step are
207 described in the following sections.

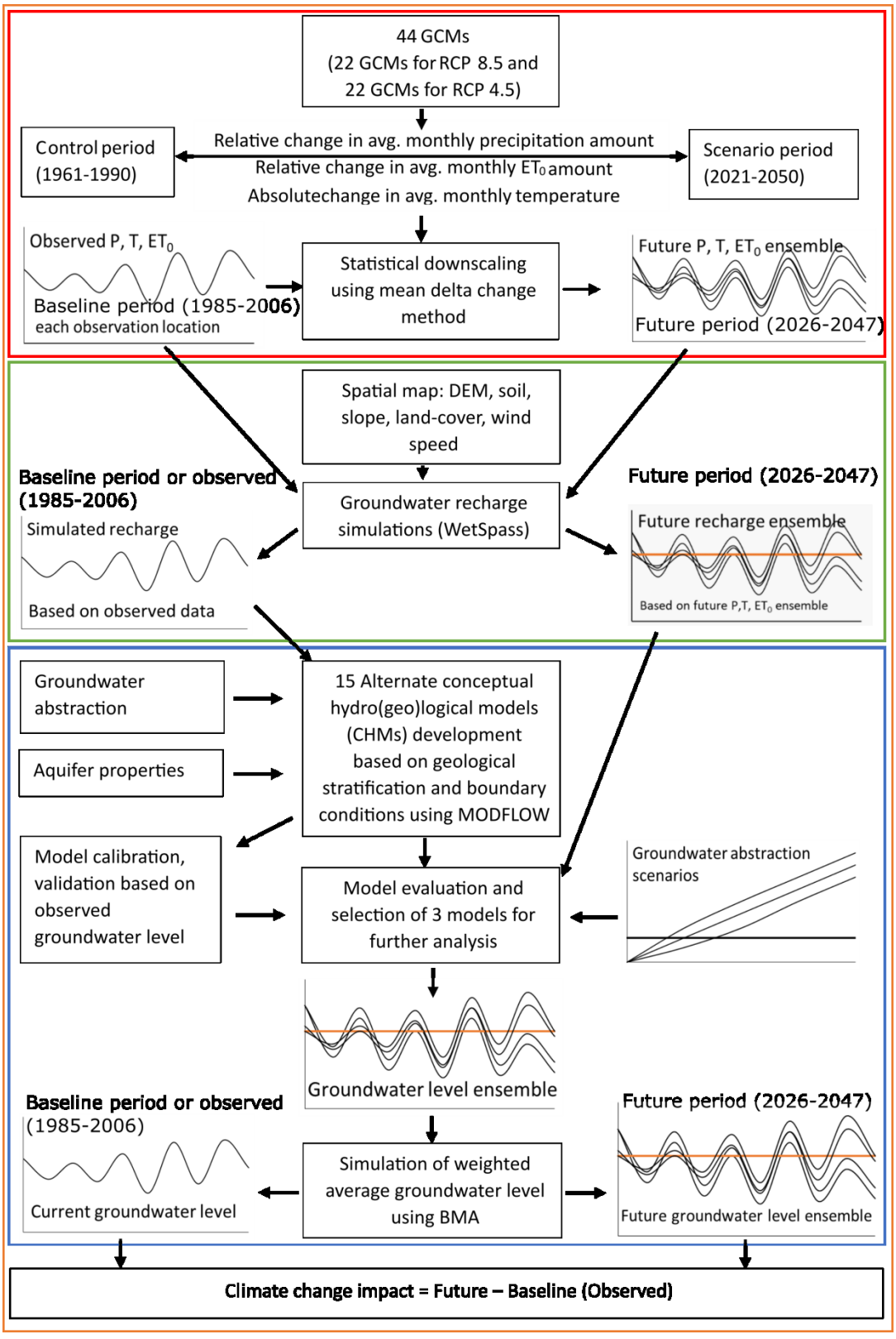
44 GCMs
(22 GCMs for RCP 8.5 and
22 GCMs for RCP 4.5)
Control period
(1961-1990)
Relative change in avg. monthly precipitation amount
Relative change in avg. monthly ET0 amount
Absolutechange in avg. monthly temperature
Scenario period
(2021-2050)
Observed P, T, ET0
Baseline period (1985-2006)
each observation location
Statistical downscaling using mean delta change method
Future P, T, ET0 ensemble
Future period (2026-2047)
Spatial map: DEM, soil, slope, land-cover, wind speed
Baseline period or observed (1985-2006)
Simulated recharge
Based on observed data
Groundwater recharge simulations (WetSpass)
Future period (2026-2047)
Future recharge ensemble
Based on future P,T, ET0 ensemble
Groundwater abstraction
Aquifer properties
Model calibration, validation based on observed groundwater level
15 Alternate conceptual hydro(geo)logical models (CHMs) development based on geological stratification and boundary conditions using MODFLOW
Model evaluation and selection of 3 models for further analysis
Groundwater abstraction scenarios
Groundwater level ensemble
Baseline period or observed
(1985-2006)
Current groundwater level
Simulation of weighted average groundwater level using BMA
Future period (2026-2047)
Future groundwater level ensemble
Climate change impact = Future – Baseline (Observed)

208

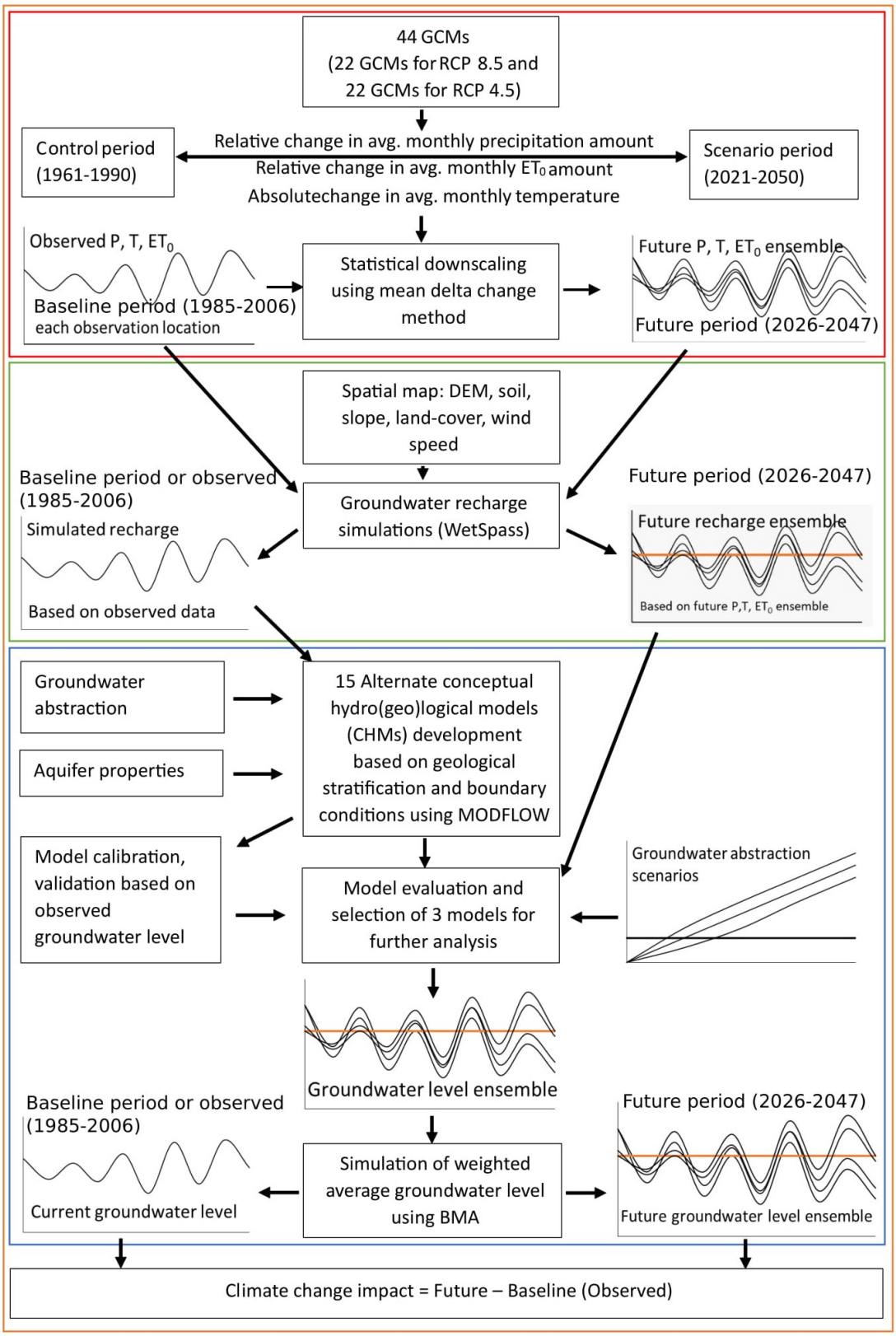

209

210 Figure 2: Multi-step multi-model methodology. GCM: General Circulation Model; RCP: Representative
211 Concentration Pathway; ET_0: potential evapotranspiration; P: precipitation; T: temperature; DEM: digital
212 elevation model; BMA: Bayesian model averaging.

213 **2.5 Alternative conceptual groundwater flow models**

214 To estimate the uncertainty due to the conceptualization of groundwater models, 15 different alternative CHMs
215 were developed based on geological stratification and boundary conditions. The cross sectional (A-A') view of
216 the models is shown in Figure 1d. First, three simplified alternative conceptual groundwater models were defined
217 based on the geological stratification. The three models are a one-layered (L1), two-layered (L2) and three-
218 layered (L3) model. In the one-layered model (L1), the entire model domain was considered as one hydro-
219 stratigraphic unit and the hydraulic properties are assumed homogeneous and isotropic. The two-layered model
220 (L2) consists of two layers where the average thickness of the top layer was 10 m (clay and loamy clay soil) and
221 rest of the thickness was considered as the bottom layer. The model domain was divided into three different
222 hydro-stratigraphic units to develop a three-layered model (L3). Below the top layer, a fine sand layer with an
223 average thickness of 8 m was added in the three-layered model. The bottom layer of three-layered model consists
224 of medium sand, coarse sand and coarse sand with gravel.

225 Boundary conditions strongly influence the CHM uncertainty (Wu and Zeng, 2013). They are often very
226 uncertain, and, moreover, strongly influence the model results. Previous studies in the Bengal basin (Michael and
227 Voss, 2009a, 2009b) identified a north to south groundwater flow direction. On the other hand, there is a large
228 wetland at the southeastern corner of the study area as well as a large river (known as Ganges/Padma) within a
229 few kilometers from the south boundary. Since exact boundary conditions were not known, based on above
230 information, five different potential sets of boundary conditions were conceptualized and shown in Figure 3. For
231 boundary condition B1, a no flow boundary condition was assumed on every side of the model. In other words,
232 there is no interaction between the model domain and the environment (Michael and Voss, 2009a, 2009b). For
233 boundary condition B2, a constant head boundary is assumed at the north side where most of the river branches
234 originated assuming that groundwater flow direction is parallel to the river flow and perpendicular to the model
235 boundary. No flow boundary conditions were assumed for all other sides. For boundary condition B3, a constant
236 head boundary was considered on the north side like for B2 and southeastern side, i.e. the side where a large
237 wetland is located. Boundary condition B4 is based on boundary condition B3. The constant head boundary in
238 the southeastern part of the model was extended to the south part of the model domain in boundary condition B4
239 because the great Ganges/Padma river is very near to the south boundary. In boundary condition B5, a constant
240 head boundary was considered at the north and northwestern boundary and also at the southeastern corner of the
241 model domain based on the information that groundwater is flowing from north and northwestern to south
242 (Michael and Voss, 2009a, 2009b). A constant head is assigned at the southeastern corner of the model domain

representing the Chalan Beel wetland as well. No-flow boundaries are assumed at the south and northeastern boundaries since these boundaries are parallel to the groundwater flow direction (Michael and Voss, 2009a, 2009b). The long-term monthly average groundwater levels (normal) were considered as the constant groundwater heads for the constant head boundary. As there is seasonal variability in the groundwater level of this study area, every month was assigned a different constant groundwater head corresponding to the long-term average groundwater level for that month.

In total, 15 alternative groundwater models were developed using 5 different boundary conditions and 3 different layer types. A list of the 15 models is included as supplementary material (Table SM-1).

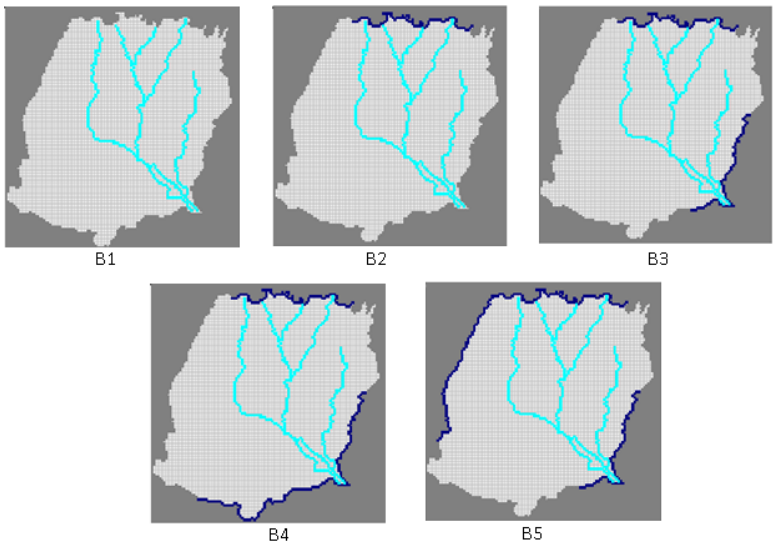

Figure 3: Boundary conditions used to develop alternative conceptual models (dark blue line indicates constant head boundary). B1: no flow boundary; B2: constant head at north boundary; B3: constant head at north and southeast boundary; B4: constant head at north, south and southeast boundary; B5: constant head at north, northwestern and southeastern boundary.

2.5.1 Model setup

The BIock Centered Flow Package (BCF) of MODFLOW-96 within the PMWIN interface was used for groundwater flow simulation. The study area covers an area of 7112 km^2 discretized into smaller cells having 117 rows and 118 columns. The grid cell dimension is 900 m x 900 m. All models are transient with a monthly time step. A no-flow boundary is considered at the model domain bottom as the vertical groundwater flow is restricted by the relatively impermeable hard rock below the aquifer in the study area. On the model top surface, a spatially distributed recharge boundary is considered.

The initial groundwater heads correspond to a long-term average groundwater table obtained by running the models in steady state conditions.

The range of hydrogeological parameter values was selected based on typical values for aquifer materials (Domenico and Mifflin, 1965; Domenico and Schwartz, 1998; Johnson, 1967) and previous research findings in the study area (Michael and Voss, 2009a, 2009b). They are listed in supplementary materials. Michael & Voss (2009b) used 9.4×10^{-5} m^{-1} as specific storage value for Bengal basin. The initial specific storage was taken as 9.4×10^{-5} m^{-1} when it is within the specific storage limits of the aquifer materials according to literature. Otherwise, the initial specific storage was taken as the average of the maximum and minimum value of the aquifer materials found in literature. The rivers in the study area are typically small and mainly driven by precipitation runoff. Generally, there is no flow in the rivers during dry months (January to March). The "River flow package" of MODFLOW was used to define rivers in the model domain and a third type boundary condition was assumed for the rivers. Riverbed conductance is indeed defined as a lumped parameter in MODFLOW defined as:

$$CRIV = \frac{K_{riv} \times L \times W}{M_{riv}} \quad (1)$$

~~$CRIV = \frac{K_{riv} \times L \times W}{M_{riv}}$~~

Where, CRIV= Riverbed hydraulic conductance (L^2T^{-1}), K_{riv} = riverbed sediment hydraulic conductivity (LT^{-1}), L = Length of the river within a grid cell (L), W = Width of the river within a grid cell (L) and M_{riv} = Thickness of the riverbed within a grid cell (L).

From the equation, it is clear that riverbed hydraulic conductance depends on grid-size, riverbed sediment hydraulic conductivity and thickness of the riverbed. Mehl and Hill (2010) have reported that riverbed conductance depends heavily on grid-size of the model. Due to lacking field data for river bed materials, the river bed conductance was obtained through manual calibration: river bed conductance is 0.18 m^2/s while riverbed thickness is 0.5 m.

2.5.2 Simulation of spatially distributed groundwater recharge

Spatially distributed monthly groundwater recharge was simulated using the WetSpass-M model (Abdollahi et al., 2017; Batelaan and De Smedt, 2001) on the same grid as the groundwater flow (MODFLOW) model. WetSpass-M is a physically based distributed model, in which the groundwater recharge is estimated from a grid-based water balance. To allow land cover heterogeneity within each cell, every raster cell is split into four

fractions: vegetated, bare-soil, open-water and impervious. The water balances of each fraction are used to calculate the total water balance of a raster cell, whereas recharge is calculated as the residual term of the water balance for each cell. The inputs of the model are spatially distributed maps of land cover, soil texture, topography, groundwater depth and climatic data. Precipitation (including of rainy days), ET_0, temperature and wind speed were used as climatic information. Details on model setup and data preparation for groundwater recharge calculation data can be found in Mustafa et al. (2017a). Monthly groundwater recharge was simulated for twenty-two years (1985-2006) and considered as the baseline groundwater recharge.

2.5.3 Groundwater abstraction estimation

Groundwater abstraction for irrigation was calculated from the available data. Unfortunately, detailed groundwater abstraction information e.g. amounts of water pumped from individual wells, co-ordinates of the abstraction wells, capacity of the pumps or duration of pumping were not available. Hence, the groundwater abstraction was assessed based on the irrigated area by shallow tube wells (STWs), deep tube wells (DTWs) and other irrigation equipment. Upazila-wise (an upazila is the second lowest tier of regional administration in Bangladesh) yearly seasonal groundwater abstraction for irrigation from the groundwater was calculated using an empirical equation based on Boro rice irrigation requirements and the irrigated area. The irrigation water withdrawal was considered as the total abstraction for each upazila. To obtain monthly abstraction for each upazila, the calculated seasonal abstraction values are initially equally divided over the months of the dry seasons (November to April). Also, as the location of the pumps is unknown, the total abstraction from each upazila is initially considered uniformly distributed over the full upazila. Considering the individual upazila as one zone of abstraction, a total of 34 abstraction zones were considered. Details on the irrigation data can be found in Mustafa et al. (2017a) and Shamsudduha et al. (2015).

2.5.4 Calibration and validation of alternative CHMs

All alternative CHMs were calibrated for the period 1990-1994. Model parameters were estimated using manual calibration and automatic calibration. During auto-calibration, PEST (Doherty, 1994) was used to optimize the model parameter values.

The initial values, allowable ranges and optimized values of the parameters of the different models are given as supplementary materials (Table SM-2, SM-3, SM-4). One-layered type models were calibrated for three parameters: horizontal hydraulic conductivity, specific storage and specific yield. The two-layered and three-layered models were calibrated for respectively 8 and 12 parameters. The process of selecting initial values and

the allowable range of the different parameters is described in section 2.5.1. -The optimized horizontal hydraulic conductivity of the one-layered models varies between 4.45 $\times 10^{-03}$ m/s and 6.00 $\times 10^{-03}$ m/s. This high value of horizontal hydraulic conductivity corresponds to well-sorted coarse sand and gravel (Fetter, 2001). We consider these values to be realistic since a major portion of the aquifer consists of coarse sand and coarse sand with gravel. The average horizontal hydraulic conductivity of Bengal basin found by Michael & Voss (2009b) was also high (5 $\times 10^{-04}$ m/s). They also reported that based on the drill-log analysis horizontal hydraulic conductivity of Bengal basin may varies from 6 $\times 10^{-06}$ m/s to 3.00 $\times 10^{-03}$ m/s. The area of the Bengal basin is about 2.8$\times$ 10^5 km^2, but the study area is only a small part of the Bengal basin. Therefore, it is possible that the horizontal hydraulic conductivity is relatively higher in our study area. Bonsor et al. (2017) have also reported in their review report that aquifer materials in the Bengal basin are highly permeable. Mustafa et al. (2018) have also reported that average horizontal hydraulic conductivity of this study area is high and around 2.5 $\times$ 10^{-3} and 4.5 $\times$ 10^{-3} m/s.

Additionally, spatial variability of horizontal hydraulic conductivity has not been considered in this study. We consider an average horizontal conductivity for all individual layers. This might be another reason for high horizontal hydraulic conductivity.

The optimized specific storage of the one-layered model with boundary condition-5 (L1B5) was 4.92$\times 10^{-05}$ m^{-1}. Michael & Voss (2009b) also reported a similar specific storage value (9.4$\times 10^{-05}$ m^{-1}) for the Bengal basin. However, different conceptual models are suggesting different specific storage values within the typical values for aquifer materials depending on the number of layers and boundary conditions (Table SM-2, SM-3, SM-4).

The optimized value of specific yield varies between 0.17 and 0.35 for different conceptual models. The results are in line with previous finding of specific yield values in the area which indicate that specific yield in the study area varies between 0.08 and 0.32, having higher values in the southern part of the Barind area (Jahan et al., 1994; Mustafa et al., 2018). However, the optimized value of specific yield for some conceptual models are equal to the upper boundary of the pre-defined parameter range. This could be because of the simplified representation of hydrogeological layers and properties of the system defined in some of the conceptual models. However, even with different conceptual models, the optimized value of specific yield is equal to the upper boundary of the parameter range, indicating that the calibrated values of the specific yield could not reach the real optimum. This could be because of uncertain groundwater abstraction and recharge data in this study area. Mustafa et al. (2018) has proven that groundwater abstraction and groundwater recharge data in space and time

in this study area are highly uncertain. They have also reported that input uncertainty (uncertainties arising from groundwater abstraction and recharge) has a significant impact on the specific yield values. However, in this study, uncertainty of the input data has not been considered. Additionally, spatial and seasonal variability of the groundwater abstraction has not been considered in this study. This might be another reason for the high specific yield value. Further improvement of model calibration would require additional and more reliable groundwater abstraction and groundwater recharge data, such as time series of pumping discharge from individual wells and exact locations of all abstraction wells.

Using the optimized parameters, each of the alternative CHMs was validated for the period of 1995 to 1999.

2.5.5 Model performance evaluation

The performance of alternative conceptual groundwater models (CHMs) was evaluated using information criterions, statistical indicators and by graphical presentation of simulated groundwater levels. Root Mean Square Error (RMSE) and, ~~Model Residual (error) Variance (σ^2),~~ Nash-Sutcliffe Efficiency (NSE, Eq. 2~~1~~) and ~~Percent Bias (PBIAS, Eq. 2)~~ of the alternative CHMs were calculated using the formula reported by Moriasi et al. (2007). ~~Here, variance is defined as the mean squared error between observed and simulated value.~~ The notation of Mustafa et al. (2017b) has been followed.

$$NSE = 1 - \frac{\sum_{i=1}^{n}(O_i - S_i)^2}{\sum_{i=1}^{n}(O_i - \bar{O})^2} \quad (2~~1~~)$$

~~$$PBIAS = \left[\frac{\sum_{i=1}^{n}(O_i - S_i)*(100)}{\sum_{i=1}^{n} O_i}\right]$$~~ ~~(2)~~

Here, O_i and S_i are representing observed and simulated values respectively, $\bar{O}$ is the mean of O_i and n is the number of observations.

NSE varies from – α to +1 and is dimensionless. NSE values closer to 1 mean better simulation efficiency. NSE values > 0.7, 0.35 – 0.7, 0.0 – 0.35 and < 0.0 represent respectively, excellent, good, fair and poor performance. ~~The unit of PBIAS is percentage and values closer to zero mean better simulation capacity. Positive and negative values are indicating respectively underestimation bias and overestimation bias (Gupta et al., 1999).~~

Information criteria are often used for model ranking (Zhou and Herath, 2017). Different information criteria such as the Akaike Information Criterion (AIC), Corrected Akaike Information Criterion (AICc), Kashyap Information Criterion (KIC) and Bayesian Information Criterion (BIC) were used to evaluate the alternative CHMs.

375 The Akaike information criterion is defined as (Zhou and Herath, 2017):

$$AIC = n\ln(\sigma^2) + 2p \quad (3)$$

$$AICc = n\ln(\sigma^2) + 2p + \frac{2p(p+1)}{n-p-1} \quad (4)$$

$$\sigma^2 = \frac{SWSR}{n} \quad (5)$$

376 Where n is the number of observations (same for all models), p is the number of model parameters = NPE+1,
377 NPE is the number of process model parameters and σ^2 is the residual variance. SWSR is the sum of weighted
378 squared residuals.

379 The Bayesian information criterion (BIC) and Kashyap information criterion (KIC) are defined in Eq. (6) and
380 (7), respectively (Zhou and Herath, 2017):

$$BIC = n\ln(\sigma^2) + p\ln(n) \quad (6)$$

$$KIC = \big(n-(p-1)\big)\ln(\sigma^2) - (p-1)\ln(2\pi) + \ln|X^T\omega X| \quad (7)$$

381 Where X is the sensitivity matrix (Jacobian matrix). The weighted factor ω applies when the errors are
382 independent from each other.

383 The different information criteria values were obtained from MODFLOW by running PEST in sensitivity
384 analysis mode. The best model among the alternative CHMs has a minimum information criteria value
385 (minimum AIC or AICc or BIC or KIC) (Zhou and Herath, 2017). A posterior model probability (p_k) was
386 calculated using Eq. (8) for each information criteria method for each alternative CHMs. The posterior model
387 probability was used to select the best CHMs. The better model corresponds to a larger posterior model
388 probability (Zhou and Herath, 2017).

$$p_k = \frac{e^{-0.5\Delta_k}}{\sum_{j=1}^{K} e^{-0.5\Delta_j}} \quad (8)$$

$$\Delta_k = AIC_k - AIC_{min} \quad (9)$$

389 Where AIC_k is the AIC value for model k and AIC_{min} is the minimum AIC values of all models. The value of Δ_k
390 was also calculated for AICc, BIC and KIC.

391 **2.5.6 Bayesian model averaging**

392 Bayesian model averaging (BMA) was used to deduce more reliable predictions of groundwater levels than the
393 predictions produced by the individual groundwater models. Draper (1994) and Hoeting et al. (1999) present an
394 extensive overview of BMA. Recently, BMA has received attention of researchers of diverse fields because of
395 its more reliable and accurate predictions than other model averaging methods. Vrugt (2016) has developed a
396 model averaging MATLAB toolbox called MODELAVG for post-processing of forecast ensembles. The
397 MODELAVG has different model averaging methods including BMA and was used in this study. Details of the
398 model averaging method are described in the MODELAVG manual (Vrugt, 2016). The value of β_{BMA}

399 (maximum likelihood Bayesian weight) was used as a criterion to select the better performing models that have a
400 significant contribution in model averaging.

401 The general equation used to calculate the weighted average prediction in various model averaging strategies is
402 as follows:

$$\tilde{y}_j = \sum_{k=1}^{K} \beta_k D_{jk} \quad (10)$$

403 Where D_{jk} is the bias corrected point forecasts of each model, k= {1,……, K} is model number and j= {1,…..n}
404 is the forecast number, $\tilde{y}_j$= { $\tilde{y}_1$,…., $\tilde{y}_n$} is the weighted average forecast for jth forecast number, β ={β_1,…., β_k}
405 denotes the weight vector.

406 **2.6 Climate change scenarios**

407 The climate model data for precipitation, minimum, mean and maximum temperature are extracted for the grid
408 cells covering the reference location within the catchment. This reference location is set at 24.81° north and
409 88.95° east and is indicated by a red dot in Figure 1b. Using the FAO Penman-Monteith equation based on the
410 temperature from climate model data, ET_0 is calculated.

411 Within this case study, CMIP5 (Coupled Model Intercomparison Project Phase 5) climate model runs for RCP
412 4.5 and RCP 8.5 are considered (Taylor et al., 2012; Van Vuuren et al., 2011). RCP 8.5 is the highest RCP-based
413 greenhouse gas scenario (GHS) and considers a radiative forcing of 8.5 W/m² by 2100. The corresponding global
414 temperature rise ranges between 2.6 and 4.8°C. RCP 4.5 is a more intermediate scenario, whereby the radiative
415 forcing is limited to 4.5W/m² by 2100 and corresponding temperature rise between 1.4 and 3.1°C (IPCC, 2013).
416 The total climate model ensemble includes 44 runs, where the RCP 4.5 and RCP 8.5 sub-ensembles each include
417 22 runs. The considered climate model runs are listed in the supplementary materials (Table SM-7).

418 The goal number six of the United Nations (UN) sustainable development Goals (SDGs) states "Ensuring
419 availability and sustainable management of water and sanitation for all by 2030". Based on this information, the
420 climate change signals, are defined between 1975 and 2035, where the control and scenario period range
421 between 1961-1990 and 2021-2050, respectively. The precipitation and evapotranspiration changes are specified
422 on a relative basis, while for the temperature changes an absolute basis is considered. Using the delta change
423 method, the climate change signals are applied to the observed time series (Ntegeka et al., 2014). The delta
424 change method is a simple statistical downscaling method which applies mean monthly average changes (top
425 box of figure 2).

426 **2.7 Future groundwater recharge scenario**

427 The projected spatially distributed monthly groundwater recharge was simulated for the 44 projected time series
428 using the WetSpass-M model (Abdollahi et al., 2017; Batelaan and De Smedt, 2001) as explained in section
429 2.5.2 and in Mustafa et al. (2017a). Details about the considered climate model runs for this study are explained
430 in section 2.6 and they are listed in the supplementary materials (Table SM-7). The baseline groundwater
431 recharge was calculated for a period of 22 years (1985–2006). Future groundwater recharge was simulated for
432 the same number of years (2026–2047). Simulated groundwater recharges of the baseline period were compared
433 to the simulated future groundwater recharge to estimate the combined influence of the greenhouse gas scenarios
434 or representative concentration pathways, climate models and internal variability.

435 **2.8 Development of future groundwater abstraction scenario**

436 It is challenging to estimate future groundwater abstraction scenarios because it largely depends on human
437 activities as well as on climate. In this study, we have developed different future abstraction scenarios. The
438 groundwater abstraction data of the study area show a linearly increasing trend during 1985 to 2006 (Figure SM-
439 4: Supplementary materials). The increasing rate is different in different groundwater abstraction zones. The
440 average groundwater abstraction rate in 2006 was about five times higher than that in 1985. A similar increasing
441 trend in groundwater abstraction in the study area was also found by Mustafa et al., (2017a). Shahid (2011)
442 predicts an increasing trend in future irrigation application for Boro rice production due to climate change. He
443 also predicts that the length of Boro rice growing period may decrease in future which may lead to increased
444 cropping intensity in the area. Increased cropping intensity may increase the overall yearly groundwater
445 abstraction rate. Moreover, it is estimated that population of Bangladesh will increase from 145 million in 2008
446 to 182 million by 2030 (Qureshi et al., 2014). Thus, water use for food production will increase tremendously.
447 As groundwater is the major source of water in the study area, groundwater withdrawal rate will be much higher.

448 However, there has not been an effective groundwater abstraction policy before 2017. Recently, the Integrated
449 Minor Irrigation Policy 2017 and the Groundwater Management Law 2018 for agriculture have been proposed to
450 ensure sustainable irrigation management. Both the Integrated Minor Irrigation Policy 2017 and the
451 Groundwater Management Law 2018 have recommended to minimize the groundwater abstraction in the study
452 area to maintain sustainable groundwater abstraction. They also encourage to use surface water instead of
453 groundwater for the irrigation. Unfortunately, no quantitative or specific action for example how much
454 abstraction should be reduced, has been mentioned either in the proposed Integrated Minor Irrigation Policy

2017 or in the Groundwater Management Law 2018. The policy planning and management strategies should be updated based on the quantitative or specific information.

Groundwater abstraction can be reduced by improving agricultural water use efficiency. The agricultural water use efficiency is extremely low in Bangladesh. On average, crops use only 25–30% of applied irrigation water and the rest is lost due to inefficient irrigation systems (Karim, 1997; Mondal, 2010, 2005). Using efficient irrigation distribution and application techniques can increase agricultural water use efficiency. The BMDA has introduced a buried PVC pipe water conveyance system in the study area to increase conveyance efficiency to more than 90%, whereas the national average value is 40% (Rahman et al., 2011). Alternate Wetting and Drying (AWD) rice irrigation technique can save 30 to 70% of water compared to conventional irrigation methods (Rahman and Bulbul, 2015). Deficit irrigation in wheat cultivation in the study area can save 121–197 mm of water per season (Mustafa et al., 2017b). Food habit changes and/or crop diversification may also have an impact on crop water use efficiency.

Considering the uncertainties on the total groundwater abstraction amount, five different groundwater abstraction scenarios are developed (~~Error! Reference source not found.~~ Table 1). The first scenario is developed based on the current increasing trend. The second scenario assumes an improved irrigation water use. As such the conveyance efficiency will compensate the increasing future demand and the groundwater abstraction rate will remain constant. In other words, this scenario considers the groundwater abstraction rate for 2010. The third, fourth and fifth scenarios assume respectively 30%, 50% and 60% lower groundwater abstraction, where the groundwater abstraction rate in 2010 was considered as a basis.

Table 1: Description of future groundwater abstraction scenarios.

Groundwater abstraction scenario	Description
P_{Linear}	Linear increase of groundwater abstraction rate based on current increasing trend
$P_{Constant}$	Groundwater abstraction rate of 2010 assumed to be constant in future
$P_{Reduced\_30}$	30% less groundwater abstraction than in 2010
$P_{Reduced\_50}$	50% less groundwater abstraction than in 2010
$P_{Reduced\_60}$	60% less groundwater abstraction than in 2010

476 **2.9 Uncertainty estimation**

477 The spread of the 95% prediction interval was taken as the uncertainty band of the ensemble. The uncertainty
478 band was estimated using Eq. (11).

$$U_{band}^{n} = D_{97.5}^{n} - D_{2.5}^{n} \tag{11}$$

$$U_{avg} = \frac{1}{N}\sum_{n=1}^{N} U_{band}^{n} \tag{12}$$

479

480 Where U_{band}^{n} is the uncertainty band of a time step, U_{avg} is the average uncertainty band, N is the total number of
481 predictions, $D_{97.5}^{n}$ and $D_{2.5}^{n}$ represent the 97.5th and 2.5th percentile of the ensemble at a time step, respectively.

482 In the case of alternative CHM uncertainty quantification, the same abstraction and recharge scenarios of the
483 baseline period were used to simulate groundwater levels of the 22-year period. To quantify the recharge
484 scenario uncertainty, the groundwater level was simulated for 44 recharge scenarios by the best performing
485 groundwater flow model where the groundwater abstraction scenario was kept the same. The groundwater level
486 was simulated for 5 abstraction scenarios by the best performing groundwater flow model where the same
487 recharge scenario was used to estimate abstraction scenario uncertainty. The groundwater levels in 50
488 observation wells for a period of 22 years were used to estimate the spread of the 95% prediction interval.

489 The contribution of the different sources of uncertainty in future groundwater level prediction was calculated
490 considering all the probable combinations of the CHMs, recharge and abstraction scenarios. The average
491 prediction interval at each time step was calculated using the following equations:

$$U_{CM_{avg}}^{n} = \frac{1}{AS \times RS}\sum_{AS=1}^{AS}\sum_{RS=1}^{RS} U_{CM_{AS,RS}}^{n} \tag{13}$$

$$U_{R_{avg}}^{n} = \frac{1}{K \times AS}\sum_{K=1}^{K}\sum_{AS=1}^{AS} U_{R_{K,AS}}^{n} \tag{14}$$

$$U_{A_{avg}}^{n} = \frac{1}{K \times RS}\sum_{K=1}^{K}\sum_{RS=1}^{RS} U_{A_{K,RS}}^{n} \tag{15}$$

492 Where, $U_{CM_{avg}}^{n}$, $U_{R_{avg}}^{n}$ and $U_{A_{avg}}^{n}$ represent the average prediction interval at each time step due to CHMs,
493 recharge scenario and abstraction scenario, respectively. The K, AS and RS represent the number of CHMs,
494 abstraction scenarios and recharge scenarios, respectively. The $U_{CM_{AS,RS}}^{n}$ is the prediction interval due to different

CHMs for a particular recharge and abstraction scenario. The $U^n_{R_{K,AS}}$ and $U^n_{A_{K,RS}}$ represent the prediction interval due to different recharge scenario and abstraction scenario, respectively for a particular CHMs and abstraction/recharge scenario.

2.10 Data analysis

Details about the procedure followed for data analysis is explained in sections 2.4 to 2.9. For data analysis and plotting, different Matlab, R and Python packages were used such as Pandas (McKinney, 2010), Scipy, ggplot2, Numpy (Walt et al., 2011) and Matplotlib (Hunter, 2007). The null hypotheses for equal distributions of simulated groundwater levels of alternative CHMs were tested using two-sample Kolmogorov-Smirnov tests (Chakravarti and Laha, 1967). The nonparametric modified Mann-Kendal trend test (Hamed and Rao, 1998) was conducted to detect trends in annual groundwater level and the slope was estimated using Sen's method (Sen, 1968).

3. Results and discussion

3.1 Groundwater levels simulation

The simulated groundwater levels of each alternative groundwater flow model were compared to the observed groundwater levels as well as to the simulated groundwater levels of the other models. The null hypotheses for the equal distribution test between simulation results of alternative models in the calibration and validation period were tested (Figure 4). A significant difference (significance level of 0.05 or $p<0.05$) between most of the alternative model's simulation results was observed. This indicates that the use of different geological stratifications and boundary conditions in groundwater flow models can result in significant differences in groundwater levels prediction and confirms the finding of Rojas et al. (2010). In contrast, some of the models did not predict statistically different results.

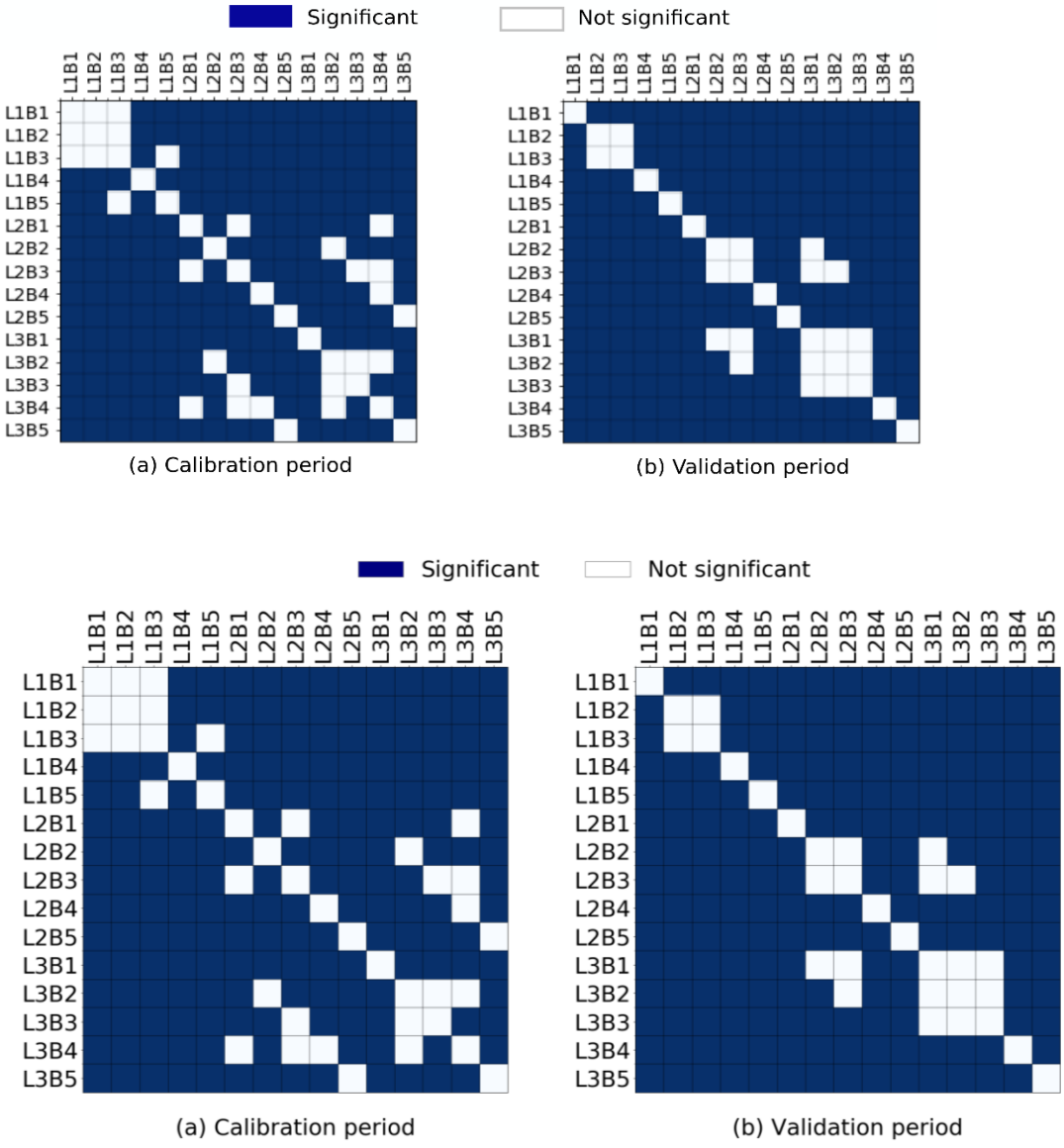

Figure 4: Significance of difference in simulation results for combinations of alternative conceptual models ($p<0.05$, two sample K-S test) for (a) calibration and (b) validation period. L1, L2 and L3 are representing respectively the one, two and three-layered model. B1, B2, B3, B4 and B5 are representing respectively Boundary condition-1,2,3,4 and 5. For example: L1B1: One-layered model with Boundary condition-1, L3B5: Three-layered model with Boundary condition-5.

3.1.1 Goodness of fit of alternative CHMs

Based on different statistical coefficients, the performance was different for alternative models, and the models performed differently in the calibration and validation period (Supplementary materials: ~~Error! Reference source not found.~~ Table SM-5).

Based on RMSE, ~~σ^2~~ and NSE value, the L2B3 model was the best model in the calibration period, whereas in the validation period it was L2B5. In general, the two-layered models had a relatively lower RMSE ~~and σ^2~~ than the one-layered and three-layered models. Overall, based on both RMSE and NSE, the two-layered models outperformed the one-layered and three-layered models in the calibration and validation period.

~~In both the calibration and validation period, PBIAS was negative for one layered models indicating that the models were overestimating groundwater head. On the contrast, two layered and three layered models generally underestimated the groundwater heads as PBIAS was positive in the calibration and validation period. The L2B5 and L2B4 model had the lowest bias in the calibration and validation period, respectively. Overall, the two-layered models outperformed the one-layered and three-layered models in the calibration and validation period.~~

The simplified one-layered models have a comparatively higher bias in prediction. Comparatively, a large number of processed parameters made the three-layered models over-parameterized. The three-layered models performed better than the one-layered models during calibration, but they performed similarly in most of the cases in the validation period. The performance of the two layered models also differed between calibration and validation period. It is difficult to calibrate over-parameterized models efficiently (Willems, 2012), so the two-layered models with eight calibrated parameters can be a balance between oversimplified and over-parameterized models.

Figure 5 shows the scatter plot for model L2B5. One of the possible causes of ~~the outliers in the scatter plot and~~ the observed differences ~~in model performance between the calibration and validation period~~ is the spatial and temporal variation in groundwater abstraction. The zone-wise spatially distributed groundwater abstraction rate was one of the most important input data in this study. In reality, groundwater abstraction varies spatially within those zones. Agricultural and industrial areas abstract more groundwater than wetlands or forest areas. Moreover, groundwater abstraction rate also ~~depends temporally~~varies in time following ~~on~~ cropping seasons and precipitation patterns. However, an average constant groundwater abstraction rate was assumed for six months (from November to April) in the model. The difference between observed and simulated are high for some observation wells. Those observation wells might be located near to abstraction wells. For observation wells close to groundwater abstraction wells, drawdown by groundwater abstraction~~,~~ could affect ~~the~~ observed groundwater heads. This spatial and temporal difference in actual groundwater abstraction and modeled groundwater abstraction causes~~d~~ spatial and temporal variation in simulated and observed groundwater levels. The simplified representation of hydrogeological layers and properties could be also a possible cause of the

differences between simulated and observed groundwater levels. For simplification, the aquifer was assumed homogeneous but in reality, the aquifer is heterogeneous and this may affect groundwater flow in the aquifer. Also, measurement errors in observation data may influence model performance.

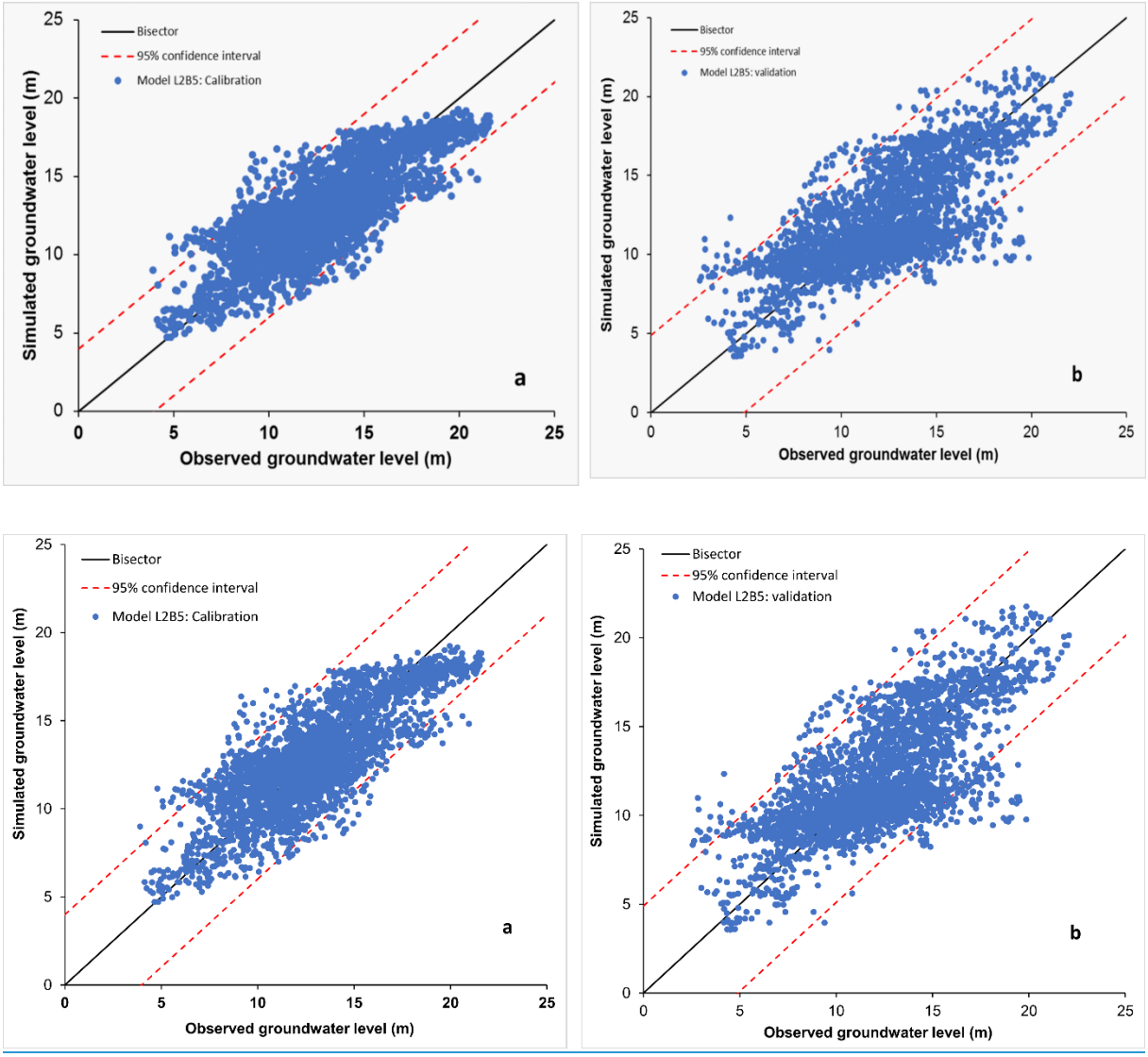

Figure 5: Scatter plot for the simulated versus observed groundwater level for Model L2B5: (a) calibration period and (b) validation period.

3.1.2 Model selection for future groundwater level simulation and uncertainty analysis

To select the best performing model, the simulation results of the calibration and validation period were used to calculate information criteria statistics. The posterior probability (p_k) was calculated using Eq. (8) for AIC, AICc, BIC and KIC methods. The L2B4 model obtained the highest posterior probability of 1, whereas all other models had negligible posterior probability for all information criteria as shown in Figure 6.

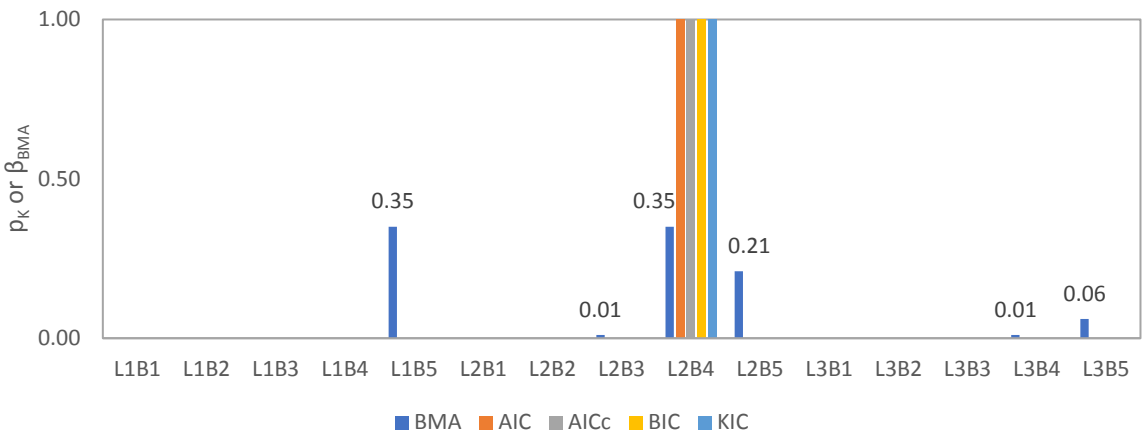

568

569 Figure 6: Posterior probability (p_k) and BMA maximum likelihood weight (β_{BMA}) of alternative models
570 calculated using 10 years of data. The value above the bar represents the maximum likelihood Bayesian weight.

571 One of the objectives was to estimate future groundwater levels using model averaging. Ten years (1990–1999)
572 of monthly simulated groundwater levels of the alternative models and observed data of 50 observation wells
573 were used as training data in MODELAVG to estimate the maximum likelihood BMA weight (β_{BMA}) of each
574 alternative model. The long training period was selected so that a reliable BMA weight can be estimated for
575 climate change impact analysis.

576 The performance evaluation statistics of BMA mean prediction along with the best model and median is shown
577 in supplementary materials (Table SM-6). The best model was selected based on the information criteria ranking.
578 The prediction of BMA method obtained better performance in all evaluation criteria than the best model and
579 ensemble median for both periods. The results are in line with the findings of Ye et al., (2004) and Poeter and
580 Anderson (2005).

581 During the training period, the 95% prediction interval covers about 85% of observed data, and the average
582 spread of the 95% prediction interval is 6.23 m. The maximum likelihood BMA weight (β_{BMA}) of all alternative
583 models is shown in Figure 6. It is observed that models L1B5 and L2B4 obtained higher β_{BMA} than other models.
584 The model L2B4 has both maximum posterior model probability and higher β_{BMA}. It is noteworthy that the L1B5
585 model obtained significant β_{BMA} as it had a comparatively poor performance in both calibration and validation
586 period compared to most of the other models. One possible cause could be the relatively better performance of
587 the one-layered model in the model boundary area.

588 Figure 6 shows that only three models (L1B5, L2B4, L2B5) together correspond to 91% of the total weight and
589 another three models (L2B3, L3B4, L3B5) correspond to 8% of the total weight. The rest of the models had no

significant contribution. The models having low β_{BMA} can be excluded from the analysis to minimize the calculation time and effort (Vrugt, 2016). Therefore, models L1B5, L2B4 and L2B5 were selected to predict future groundwater levels under different scenarios. Ultimately, β_{BMA} was recalculated using the prediction of those selected models and the new β_{BMA} of L1B5, L2B4 and L2B5 was 0.35, 0.39 and 0.26, respectively. During this recalculation, the 95% prediction interval covers about 82% of observation data meaning exclusion of 12 models resulted in a loss of only 3% of observed data.

3.2 Climate change impact on precipitation, temperature and evapotranspiration

Figure 7 shows the changes in monthly climatic parameters between the control and scenario period ranging between 1961-1990 and 2021-2050, respectively. Figure 7a shows the changes in the monthly precipitation amount. Small positive changes in monthly precipitation amounts are observed for the wet season. For the dry season (November to April), in contrary, the changes are less consistent: decreasing precipitation amounts are found for April and December while March display a significant increase. The effect of the greenhouse gas scenario (GHS) on the monthly precipitation amount changes is shown by Figure 7b. One would expect increasing/decreasing change signals under increasing GHSs. This uni-directional behavior is, however, limited to the months July, August, September and November. Most likely, 2035 is situated before the time of emergence, whereby the effect of the increasing GHS remains mainly masked by noise inherent to the internal climate variability (Hawkins and Sutton, 2012). This, moreover, indicates that the months July, August, September and November are most likely more sensitive to the GHSs compared to the other months.

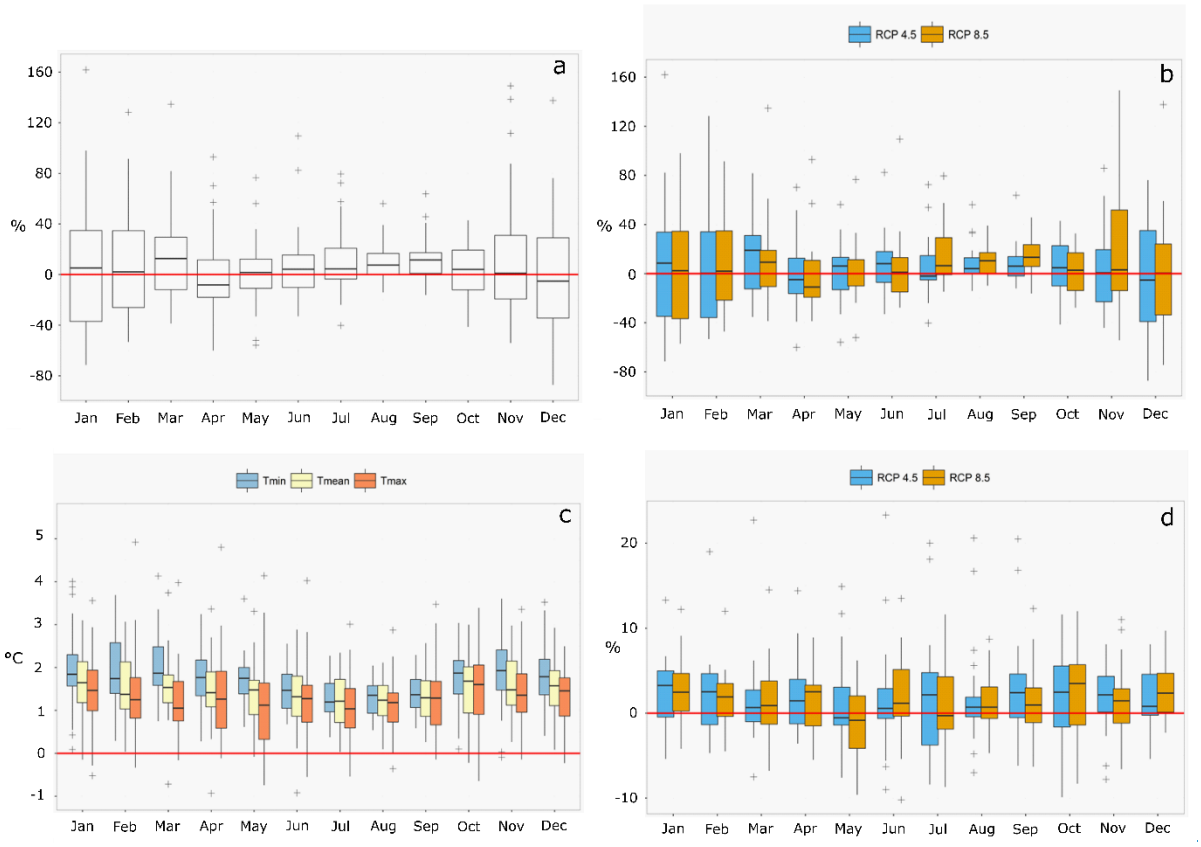
a
b
c
d
RCP 4.5
RCP 8.5
Tmin
Tmean
Tmax
%
°C
Jan
Feb
Mar
Apr
May
Jun
Jul
Aug
Sep
Oct
Nov
Dec

608

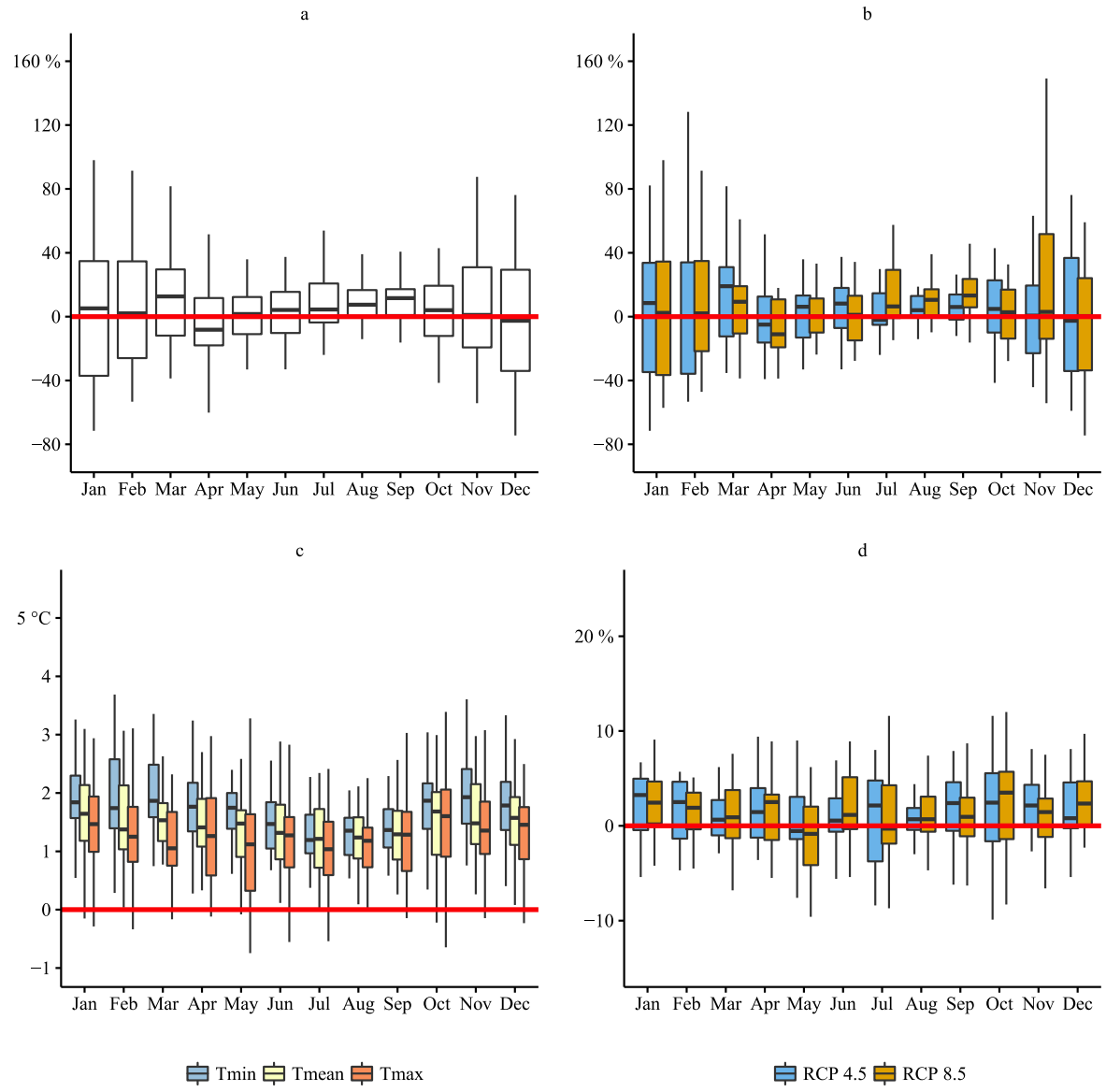

Figure 7: Climate impact signal for all selected climate models (1975 – 2035): (a) relative changes in monthly precipitation amount (all GHS combined), (b) relative changes in monthly precipitation amount as function of the GHSs, (c) absolute changes in monthly minimum, mean and maximum daily temperature (all GHSs combined), and (d) relative changes in potential evapotranspiration as function of the GHSs.

Figure 7c presents the climate scenarios for minimum, mean and maximum daily temperature. It shows the absolute changes in monthly minimum, mean and maximum daily temperature between the control and scenario period. Generally, higher increases in minimum and mean daily temperatures are projected during the wet season. An inter-comparison between the different variables shows, furthermore, higher changes for the minimum daily temperature than for the mean and maximum daily temperature.

The changes in monthly potential evapotranspiration are shown in Figure 7d. Except for May, increases are observed for all months. For some months, the changes seem not sensitive to the GHS. Changes for the months March, April, June, October and December seem particularly sensitive to the GHS. Similar as for the precipitation results, a possible explanation can be found in the "time of emergence" concept.

The climate change signals for a representative month in the dry and wet season are included in supplementary materials (Table SM-8).

3.3 Climate change impact on groundwater recharge

The changes in the monthly groundwater recharge due to climate change are highly uncertain (Figure 8a). Like precipitation, small increasing changes in monthly groundwater recharge are observed for the wet season. For the dry season (November to April), in contrary, the changes are less consistent. The majority of the global climate model runs project generally an increasing groundwater recharge. However, for April and December, significant decreases are noted. The effect of the GHSs on the monthly groundwater recharge changes is shown by Figure 8b. The months July, August, September and November seem to be more sensitive to the GHSs compared to the other months. For both RCP 8.5 and RCP 4.5, April and December show decreasing changes in monthly groundwater recharge.

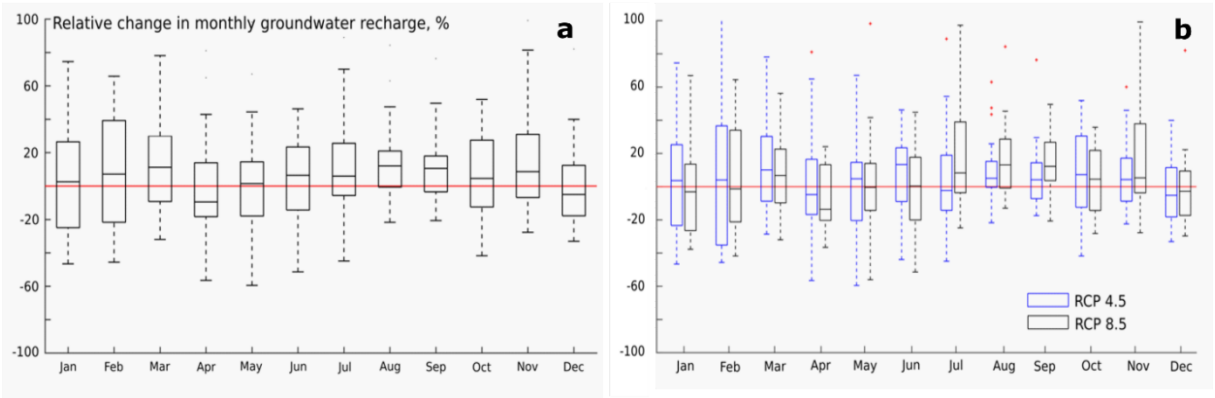

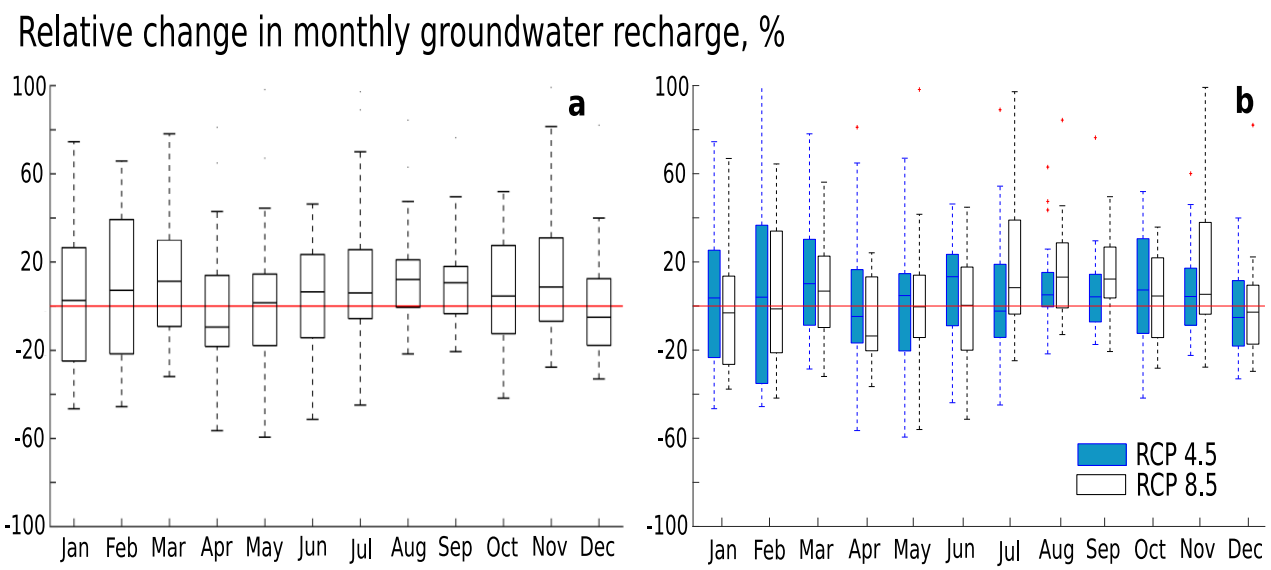

635

636 Figure 8: Change in groundwater recharge due to climate change: (a) relative changes in monthly groundwater
637 recharge (all GHS combined), (b) relative changes in monthly groundwater recharge as a function of the GHSs.

638 Projected spatial variation of the mean groundwater recharge change between the future and the baseline period
639 due to climate change is presented in Figure 9. Spatial variation is observed only for two extreme recharge
640 scenarios: high recharge scenario is indicating maximum recharge at each time step among all the ensembles and
641 low recharge scenario is indicating minimum recharge. Both for April and September, the high recharge scenario
642 shows a zero to positive change in groundwater recharge, while the low recharge scenario shows a zero to
643 negative change in groundwater recharge. No clear spatial trends are observed in the change of groundwater
644 recharge. In the high recharge scenario, mean monthly groundwater recharge would increase by 25 mm (April)
645 and 100 mm (September). In the low recharge scenario, mean monthly groundwater recharge would decrease by
646 16 mm (April) and 35 mm (September). Crosbie et al. (2010), also, reported that changes in groundwater
647 recharge due to climate change are uncertain.

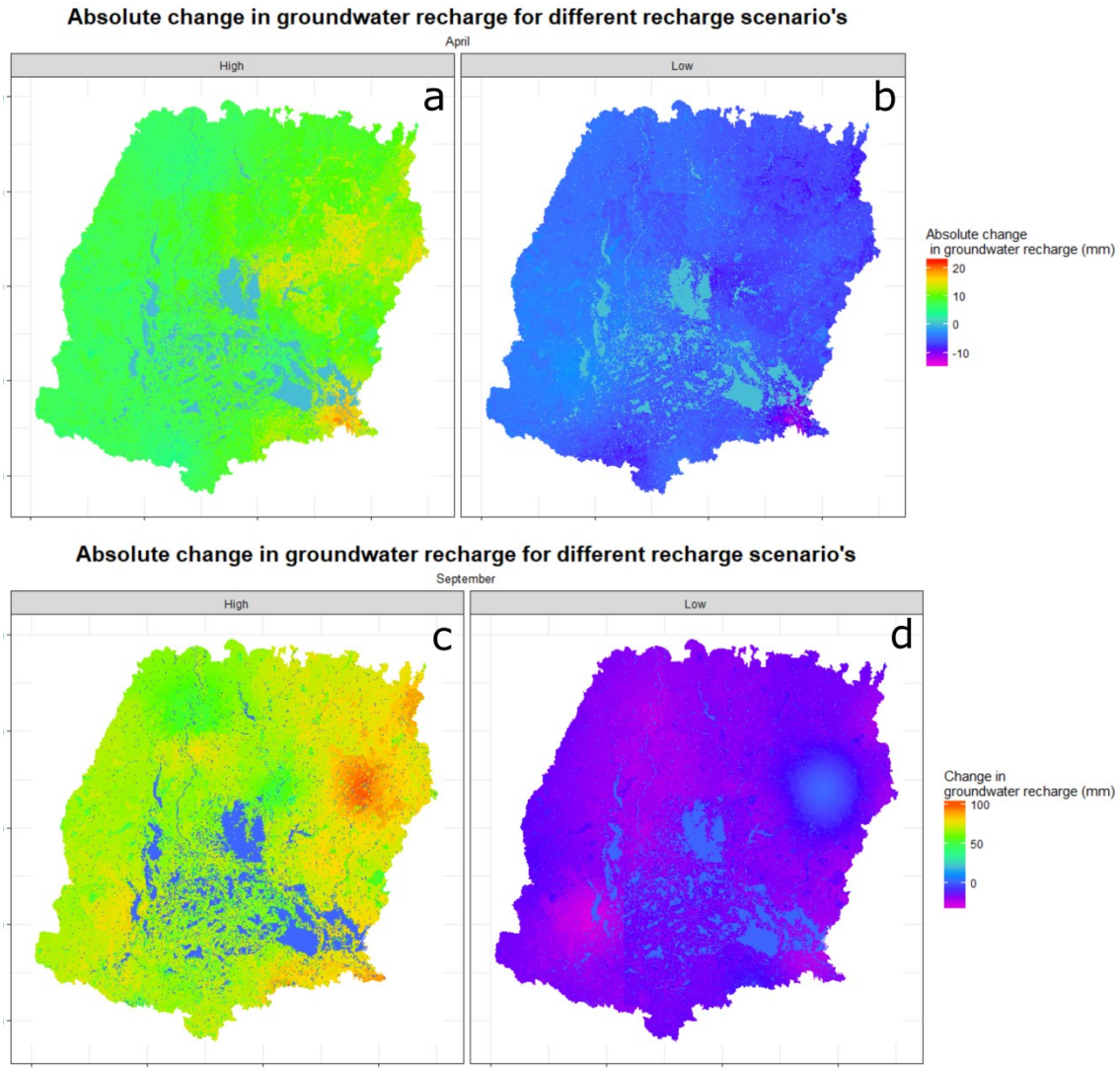

Figure 9: Spatial variation of mean groundwater recharge change due to climate change for (a) high recharge scenario in April, (b) low recharge scenario in April, (c) high recharge scenario in September and (b) low recharge scenario in September.

3.4 Future groundwater level analysis

The baseline and future groundwater levels were simulated using three selected groundwater flow models (L1B5, L2B4, L2B5). Then, the model average was calculated by Eq. (10) using simulated groundwater levels and the maximum likelihood Bayesian weight of the respective groundwater flow models. The change in groundwater level for different scenarios is discussed below.

3.4.1 Baseline groundwater level simulation

Groundwater levels in the baseline scenario show a decreasing trend. The mean decreasing rate of groundwater level is 0.18 m/year (Sen's slope). The summary of the trend analysis for 50 observation wells is shown in

660 supplementary materials (Table SM-9). The calculated decreasing rate varies spatially and ranges between 0.05
661 to 0.49 m/year. Mustafa et al. (2017a) studied observed groundwater level data of the same study area and
662 reported that the average groundwater level dropped by 4.5–4.9 m over the last 29 years at a rate of 0.15–0.17
663 m/year. The annual groundwater level fluctuation of 3 to 5 m in the baseline scenario is also supported by the
664 findings of Shamsudduha et al. (2009). Overall, the simulated groundwater levels correspond well with the
665 findings of other researchers for the baseline period. Therefore, the simulated groundwater level of the baseline
666 period was used for comparison with the simulated groundwater levels of the future scenarios.

667 **3.4.2 Impact of climate change on groundwater level**

668 Impact of climate change on groundwater level is highly uncertain in the study area (Figure 10a). The
669 uncertainty ranges of the change in mean monthly groundwater level due to different GCMs and GHSs obtained
670 from the three selected conceptual groundwater flow models are presented with the box-plot for each month.
671 Climate change could increase the mean monthly groundwater level by up to 2.5 m and could decrease by 0.5 m.
672 However, the SDGs suggest 0-0.5 m increase in groundwater level due to climate change. The impact of climate
673 change seems higher from May to September than from October to April. This seasonal variation of climate
674 change impact can be explained by the precipitation pattern of the study area (Supplementary materials: Figure
675 SM-2a). Large precipitation amounts occur from May to October in Bangladesh, so that climate change has a
676 higher impact on this period. Uncertainty of groundwater level due to climate change is highest from June to
677 December. The precipitation pattern can also explain the monthly variation of climate change impact
678 uncertainty. Groundwater levels increase more during the rainy season in a high recharge scenario (high
679 precipitation), but in a low recharge scenario, groundwater levels decrease due to the lack of recharge in the
680 rainy seasons. Therefore, the uncertainty band increases in this period for extreme scenarios. Similar to
681 precipitation and groundwater recharge, the effect of the GHSs are not very significant on groundwater level
682 changes (Figure 10b). Most of the GCMs project that the increase of groundwater level would be higher for RCP
683 8.5 compared to RCP 4.5 for all months.

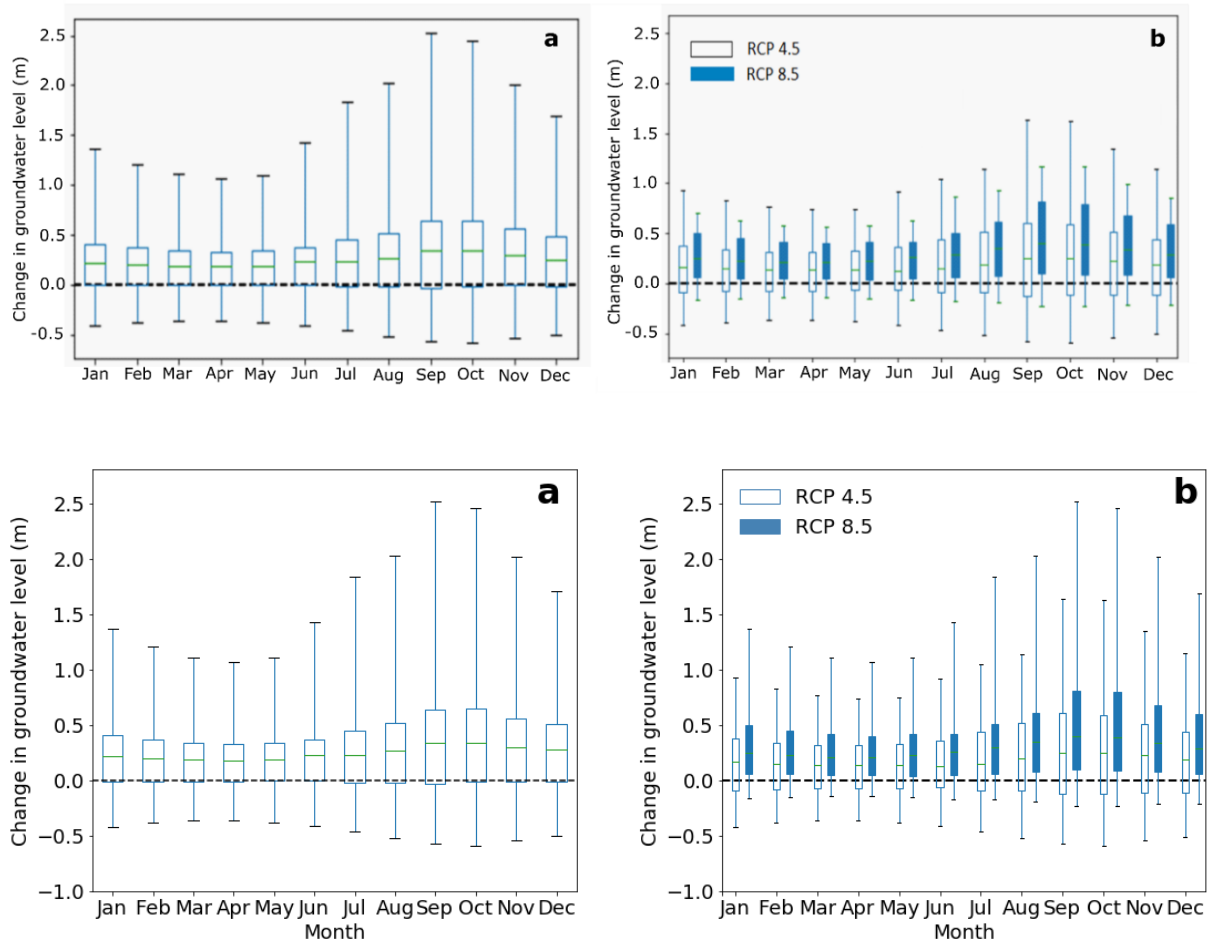

Figure 10: Mean monthly change of groundwater levels in the simulated future period (2026-2047) compared to the baseline period (1980-2006) due to climate change: (a) all GHS combined, (b) as a function of the GHSs.

The impact of climate change on groundwater level also varies spatially. The projected impact of climate change on groundwater level is relatively higher in the southwestern part (Figure 11) although this pattern does not correspond to the spatial pattern of groundwater recharge (Figure 9). This can be explained by the effect of the river on groundwater level. In a high recharge scenario mean monthly groundwater level would increase up to 4 m (April) and 8 m (September). However, in a low recharge scenario, mean monthly groundwater level would decrease up to 1.6 m. Overall, the impact of climate change on groundwater level was not linear.

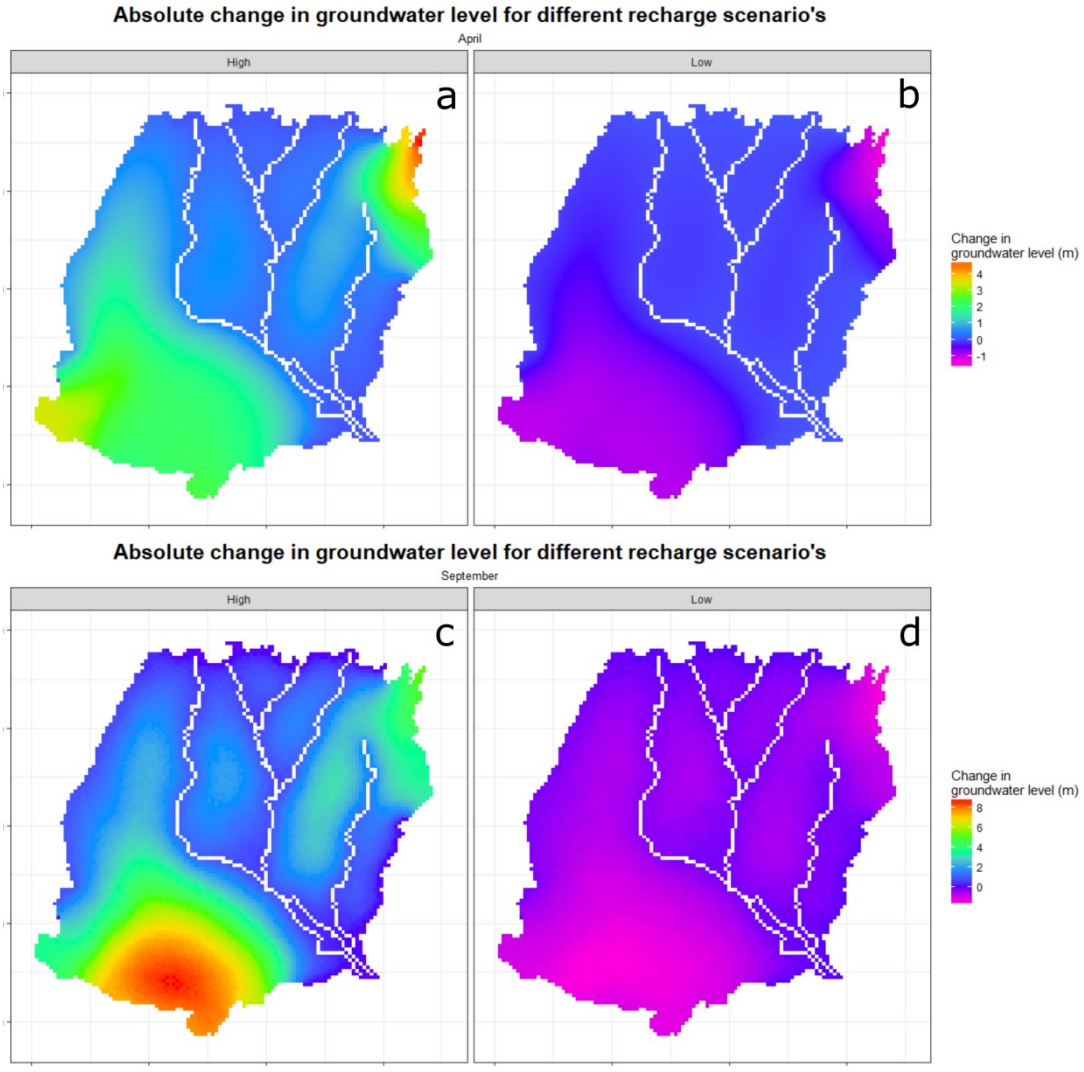

Figure 11: Spatial variation of mean groundwater level change due to climate change for the (a) high recharge scenario in April, (b) low recharge scenario in April, (c) high recharge scenario in September, and (b) low recharge scenario in September.

3.4.3 Future groundwater level under different abstraction scenarios

The mean monthly groundwater level for the P_{Linear} abstraction scenario decreases about 10 to 14 m compared to the baseline period (Figure 12a). The scenario of $P_{Constant}$ resulted in a 4 to 7 m decrease in groundwater level (Figure 12b). For the 30% reduced ($P_{Reduced\_30}$) abstraction scenario, the mean groundwater level would decrease about 1.5 to 3.8 m (Figure 12c). Even for the 50% reduced ($P_{Reduced\_50}$) abstraction scenario, the mean groundwater level would decrease about 1.0 to 1.5 m (Figure 12d). Groundwater abstraction in the study area has to be reduced by 60% compared to the groundwater abstraction rate in 2010, to keep a sustainable groundwater level (Figure 12e). This indicates that the groundwater abstraction rate of 2010 is much higher than the future recharge potential. The situation will be worse if the current increasing groundwater abstraction trend continues.

A spatial variation in groundwater level change for different abstraction scenarios was also observed. In a low recharge scenario, even for a 30 % reduced ($P_{Reduced\_30}$) abstraction scenario, groundwater level decreased about 14 m in the southwestern part of the study area. In a high recharge scenario, on the other hand, groundwater level increased about 2 m in the northeastern part of the study area for the $P_{Reduced\_30}$ abstraction scenario. The results also show that 50% lower groundwater abstraction than the 2010-rate is not enough to stop groundwater level declining in the southwestern part of the study area.

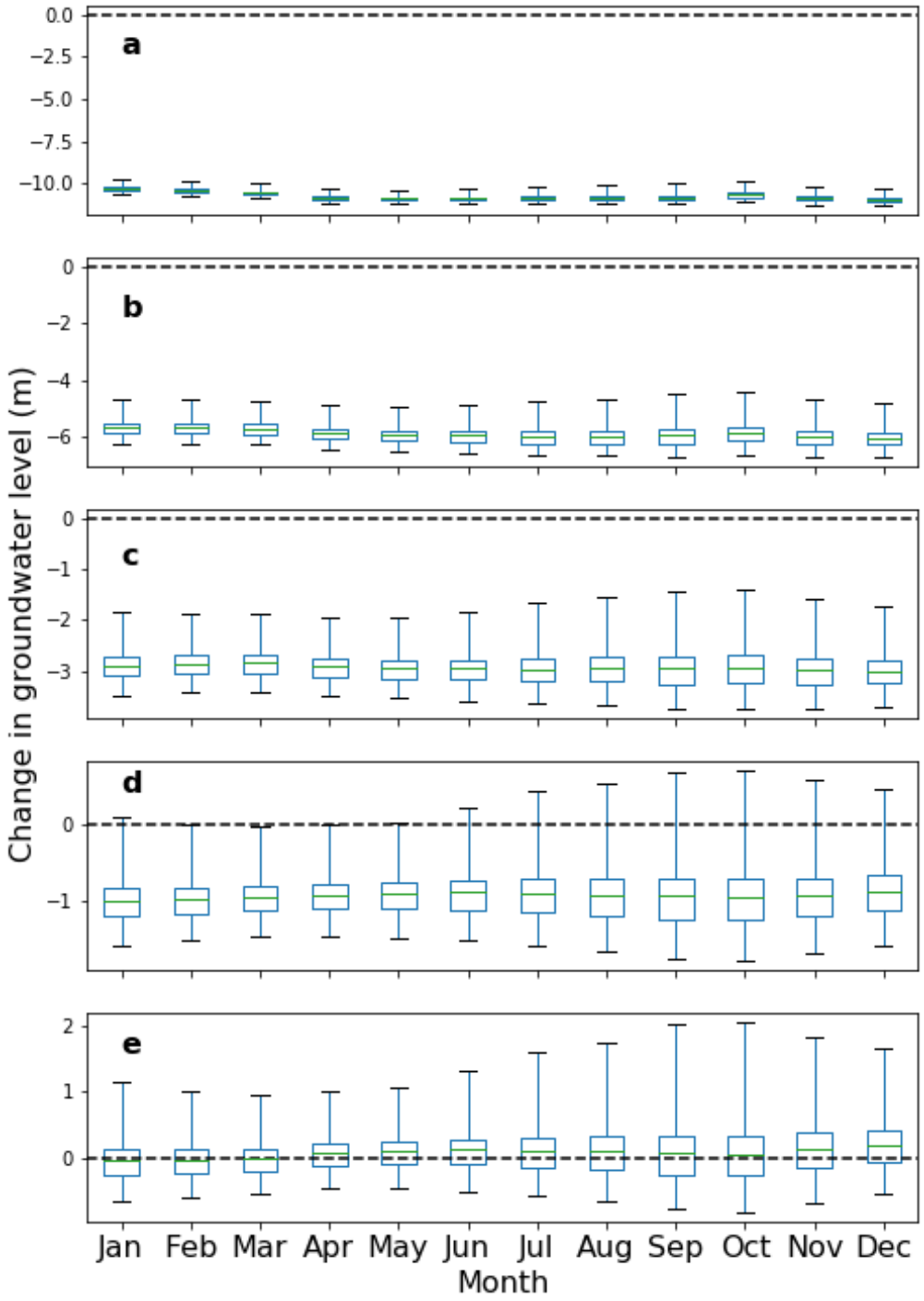

Figure 12: Monthly mean change in groundwater levels in the simulated future period (2026-2047) compared to the baseline period (1985-2006) due to groundwater abstraction: (a) for P_{Linear} abstraction scenario; (b) for $P_{Constant}$ abstraction scenario; (c) for 30 % reduced ($P_{Reduced\_30}$) abstraction scenario; (d) for 50 % reduced ($P_{Reduced\_50}$) abstraction scenario and (e) for 60 % reduced ($P_{Reduced\_60}$) abstraction scenario.

The summary of annual groundwater level trend analysis of 50 observation wells for the high and low recharge scenario and for different abstraction scenarios (P_{Linear}, $P_{Constant}$, and $P_{Reduced\_30}$) is shown in Table 2. Only the significant ($p<0.05$) trends were considered in this analysis. Scenario $P_{Constant}$ and $P_{Reduced\_30}$ have a mean decreasing rate that is two to three times higher than the baseline scenario. Therefore, proper groundwater abstraction policy is necessary to maintain sustainable use of this resource.

Table 2: The summary of annual groundwater level trend statistics of 50 observation wells for the baseline (1985–2006) and simulated future (2026–2047) period under different abstraction scenarios (P_{Linear}, $P_{Constant}$, $P_{Reduced\_30}$) and recharge scenarios (Low, High).

	Baseline period	Simulated future period					
		P_{Linear}		$P_{Constant}$		$P_{Reduced\_30}$	
		Low	High	Low	High	Low	High
Statistics	Slope (m/year)						
Mean	-0.18	-1.10	-1.02	-0.50	-0.47	-0.37	-0.30
Maximum	-0.05	-0.06	-0.06	-0.03	-0.04	-0.04	-0.09
Minimum	-0.49	-3.89	-3.71	-1.88	-1.54	-1.13	-0.79
Median	-0.15	-0.39	-0.38	-0.37	-0.35	-0.27	-0.18
Standard deviation	0.11	1.23	1.12	0.51	0.40	0.29	0.25

3.5 Sources of uncertainty in groundwater level prediction

3.5.1 Alternative conceptual model (CHMs) uncertainty

The 95% prediction intervals of the three best performing models are shown in Figure 13a. The average spread of the 95% prediction interval of the three alternative CHMs was about 3 m with a maximum spread of about 16 m. It is observed that the spread of the prediction interval is wider for low and high groundwater levels. This is not surprising as the one-layered model overestimates low groundwater levels and underestimates high groundwater levels in most of the observation wells. The wide uncertainty band of the alternative CHMs indicates that the use of a single model in groundwater levels prediction may lead to biased conclusions.

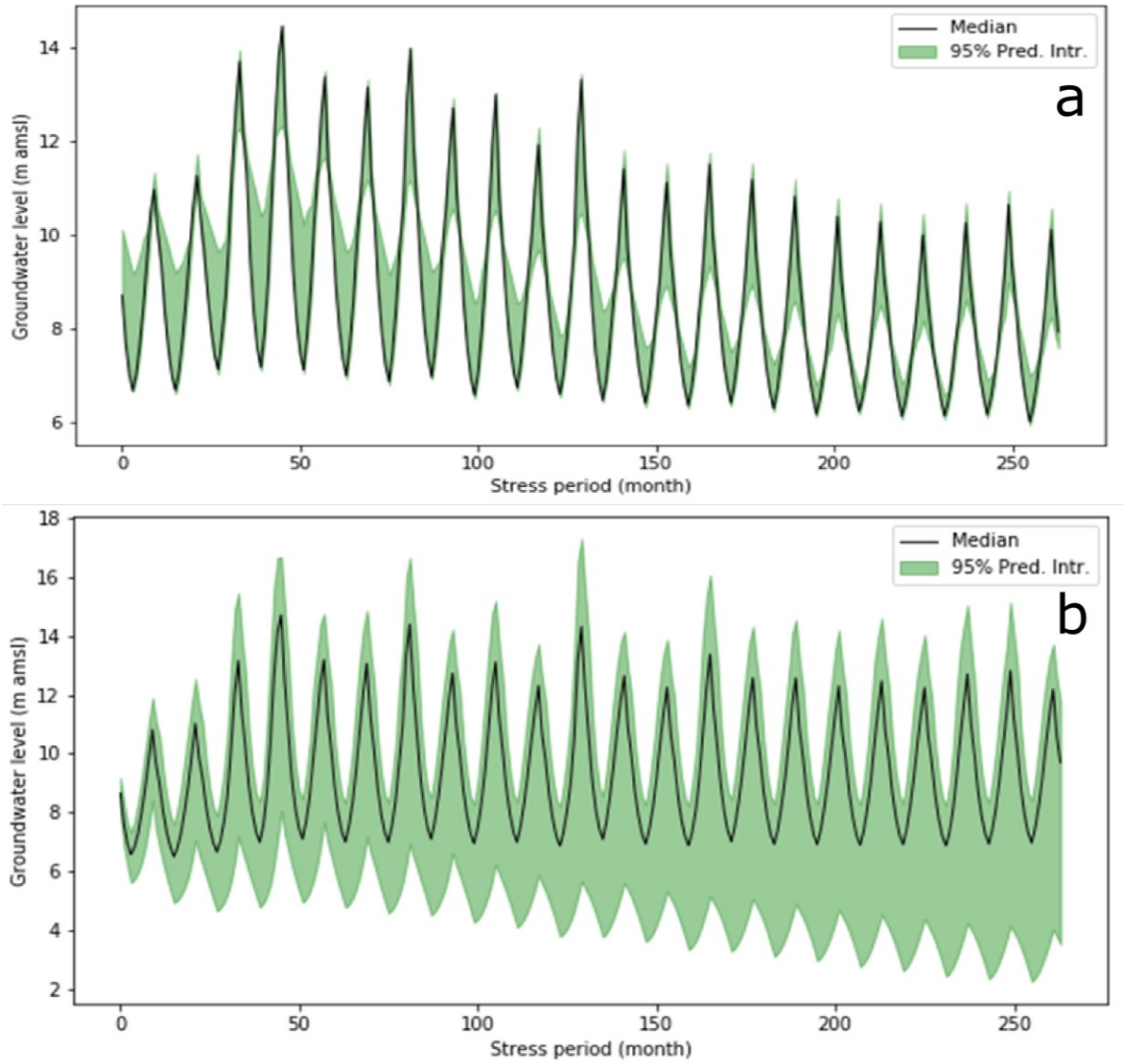
Median
95% Pred. Intr.
a
Groundwater level (m amsl)
Stress period (month)
Median
95% Pred. Intr.
b
Groundwater level (m amsl)
Stress period (month)

735

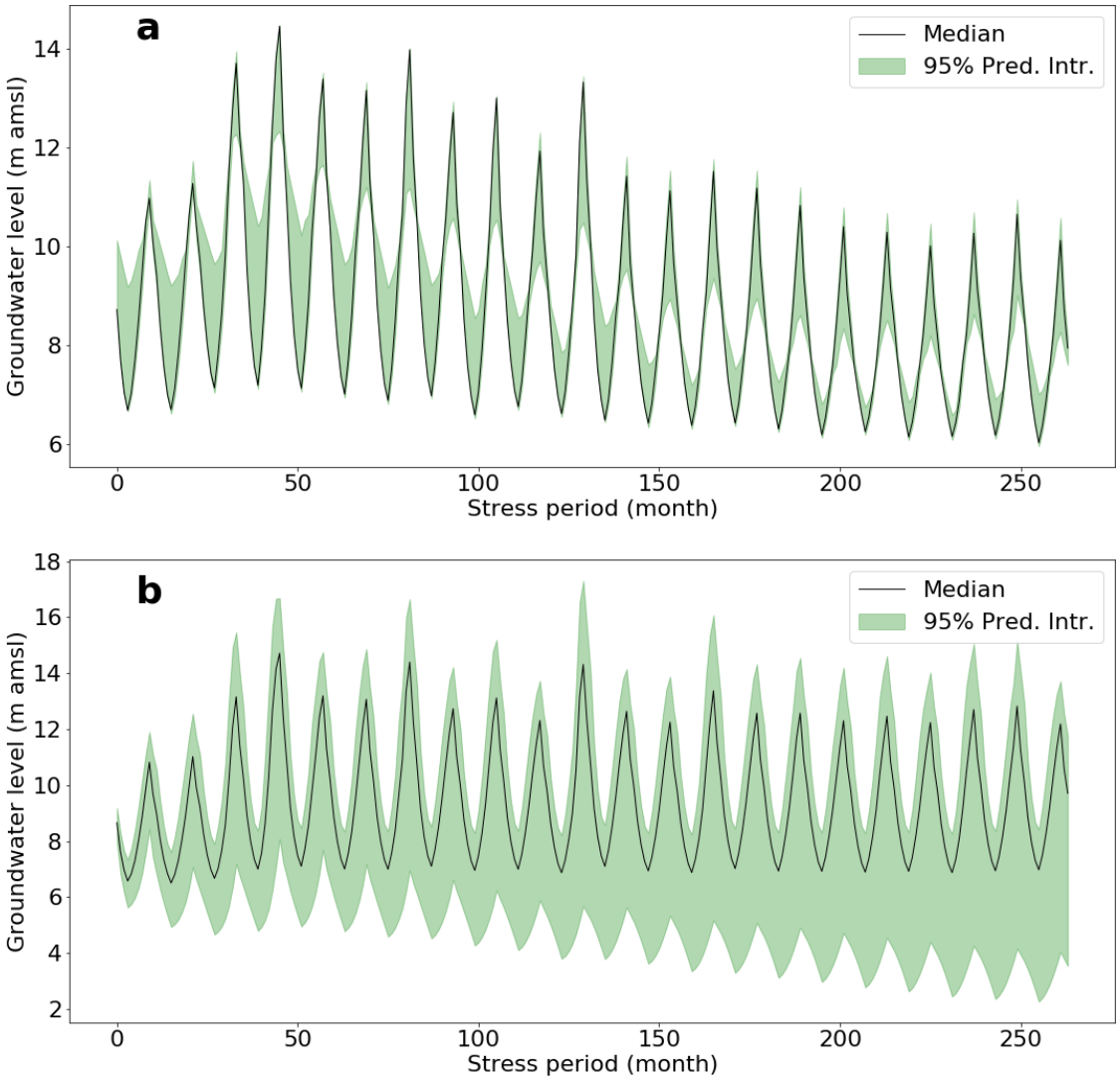

Figure 13: The 95% prediction interval of groundwater level of a representative observation well (BOG001) for (a) different conceptual models and (b) different abstraction scenarios.

3.5.2 Recharge scenarios uncertainty

The average spread of the 95% prediction interval due to recharge scenarios is 1.11 m with a maximum of 6.07 m. The predictive uncertainty due to the recharge scenario is higher during periods with high groundwater levels and recharge. Although the mean uncertainty resulting from recharge scenarios is relatively lower than for other sources of uncertainty, there is large temporal and spatial variation in groundwater level prediction due to recharge scenarios (as described in section 3.4.2). The recharge scenarios were developed using future climate scenarios of different climate models so that the uncertainty from recharge scenarios represents the uncertainty

746 from climate scenarios in groundwater levels prediction. This uncertainty analysis suggests that all possible
747 climate scenarios should be considered to predict groundwater levels with a reliable uncertainty band.

748 **3.5.3 Abstraction scenarios uncertainty**

749 The 95% prediction interval of groundwater level for different abstraction scenarios increases with time (Figure
750 13b). The average spread of the 95% prediction interval is 8.38 m and the maximum is 43 m. The uncertainty of
751 groundwater level related to the abstraction scenario is very high.

752 **3.5.4 Comparison of sources of uncertainties**

753 The uncertainties due to alternative CHMs, recharge scenarios and abstraction scenarios are compared (Figure
754 14). The spread of the prediction interval of groundwater levels resulting from different CHMs, recharge
755 scenarios and abstraction scenarios was estimated using Eq. (13), (14) and (15), respectively. The contribution of
756 each source was calculated based on the median value of the spread of the prediction interval. The contribution
757 of an individual source is calculated as the ratio of the median value of the spread of the prediction interval for
758 the respective source to the median value of the spread of the prediction interval for the total uncertainty. The
759 abstraction scenarios are the dominant source of the total uncertainty in groundwater level prediction in this
760 overexploited aquifer. About 68% of the total uncertainty arises from the abstraction scenarios. CHM uncertainty
761 contributed about 23% of total uncertainty. This result is in agreement with the findings by Rojas et al. (2008).
762 They reported CHM uncertainty contributions up to 30%. In this case, the alternative CHM uncertainty
763 contribution is higher than the recharge scenario uncertainty contribution, including the greenhouse gas scenario,
764 climate model and stochastic climate uncertainty contributions. Goderniaux et al. (2015) reported that
765 uncertainty related to the calibration of hydrological models can be more important than uncertainty related to
766 climate models in groundwater modeling. The uncertainty due to recharge scenarios was relatively lower than
767 the other sources but the uncertainty arising from recharge scenarios was very high in the southwestern part of
768 the study area (described in section 3.4.2). Hence, use of a single model or single recharge or abstraction
769 scenario may lead to biased estimation of groundwater levels. Therefore, a multi-model and multi-scenario
770 approach should be used for reliable groundwater levels prediction.

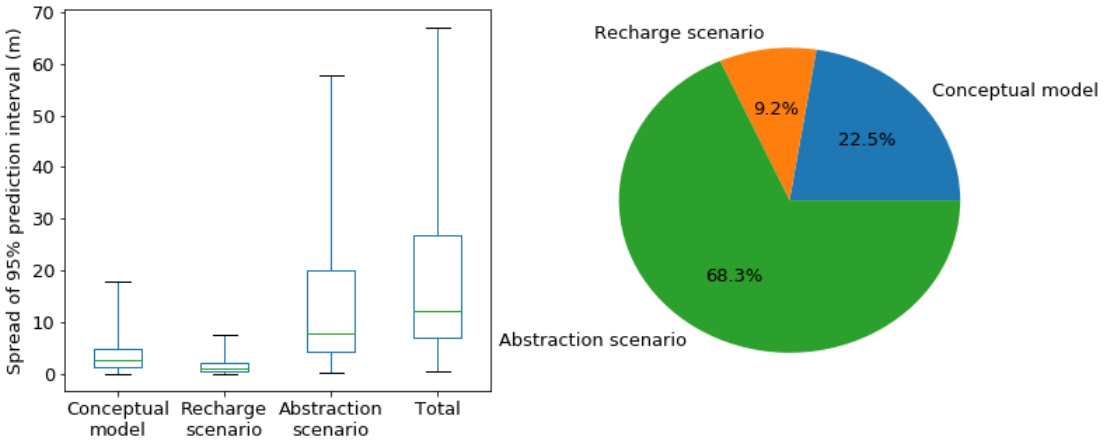

771

772 Figure 14: Comparison of uncertainties arising from alternative conceptual models, recharge scenarios and
773 abstraction scenarios. The recharge scenario uncertainty includes the greenhouse gas scenario uncertainty, the
774 climate model uncertainty and the stochastic uncertainty.

775 **4 Conclusions**

776 The main objective of this study was to quantify groundwater level prediction uncertainty in climate change
777 impact studies using an ensemble of representative concentration pathways, global climate models, multiple
778 alternative CHMs and abstraction. In this study, 15 alternative CHMs, 22 climate model runs for representative
779 concentration pathways 4.5 and 8.5 (in total 44 climate model runs) and 5 groundwater abstraction scenarios
780 were used to achieve this aim. The BMA technique was used to predict reliable groundwater level using
781 predictions of alternative CHMs.

782 It was observed that different conceptual groundwater models (CHMs) can simulate significantly different
783 groundwater levels due to differences in the number of layers and the boundary conditions. The simple one-
784 layered models were unable to simulate seasonal variation, but had a relatively better performance close to the
785 model boundaries than the other multi-layered models. The three-layered models were more detailed, but the
786 performance was not superior to the two-layered models. The performance of the two-layered models was
787 mostly better than the one-layered and three-layered models.

788 Ranking of models differed in the calibration and validation period. The best model in the calibration period only
789 got the 4th rank in the validation period suggesting the importance of the use of multiple CHMs for reliable
790 prediction.

The impact of groundwater abstraction on groundwater levels is very high. For 2026–2047, the groundwater level would decline about 5 to 6 times faster than in the baseline period (1985–2006) if the current increasing groundwater abstraction trend continues. Even with a 30% lower groundwater abstraction rate compared to the 2010-rate, the mean monthly groundwater level would decrease by up to 14m in the southwestern part of the study area. Groundwater abstraction has to be reduced by 60% compared to the 2010-rate to keep groundwater level sustainable. This indicates that the groundwater abstraction rate of 2010 was far higher than recharge potential.

The differences in groundwater abstraction scenarios were the dominant source of uncertainty in groundwater level prediction. The uncertainty due to alternative CHMs was also found to be significant and higher than the uncertainty from the recharge scenarios. The uncertainty due to different recharge scenarios was very high in southwestern part of study area. Therefore, use of a single model and/or single recharge and abstraction scenario can lead to biased groundwater levels prediction.

This study suggests that a multi-model approach should be used in groundwater level prediction to avoid biased estimation of groundwater levels. The BMA is probably the most suitable technique for developing a multi-model average based on the best available data and future alternative scenarios. This study recommends that the uncertainty due to alternative CHMs, recharge and abstraction scenarios should be considered in future groundwater levels prediction.

In this study, alternative conceptual models have been calibrated using PEST. However, different calibration methods can result in different calibrated model parameters. Hence, further studies could be conducted using different calibration methods (e.g. global parameters optimization methods). We also advice that more field data would be collected, such as reliable groundwater abstraction data, river flow information, spatially distributed horizontal hydraulic conductivity and detailed information about the boundary conditions.

Keeping in mind that the complexity of hydrogeological models is increasing, further studies should be conducted on global sensitivity analysis (SA) to (i) identify the influential and non-influential parameters on the model prediction and (ii) better understand the importance of the different components of the complex model structure. Identification of influential parameters will play an important role in model parameterization and in reducing uncertainty due to overparameterization. The identification of non-influential parameters using SA will be a very important step in simplifying model structure.

Acknowledgements

We acknowledge the World Climate Research Programme's Working Group on Coupled Modelling, which is responsible for CMIP, and we thank the climate modeling groups for producing and making available their model output. The 5th author obtained a PhD scholarship from the Fund for Scientific Research (FWO)-Flanders. This financial support is gratefully acknowledged.

References

Abdollahi, K., Bashir, I., Verbeiren, B., Harouna, M.R., Van Griensven, A., Huysmans, M., Batelaan, O., 2017. A distributed monthly water balance model: formulation and application on Black Volta Basin. Environ. Earth Sci. 76, 198.

Ali, R., McFarlane, D., Varma, S., Dawes, W., Emelyanova, I., Hodgson, G., Charles, S., 2012. Potential climate change impacts on groundwater resources of south-western Australia. J. Hydrol. 475, 456–472.

Allen, R.G., Pereira, L.S., Raes, D., Smith, M., 1998. Crop evapotranspiration-Guidelines for computing crop water requirements-FAO Irrigation and drainage paper 56. FAO Rome 300, D05109.

Asad-uz-Zaman, M., Rushton, K.R., 2006. Improved yield from aquifers of limited saturated thickness using inverted wells. J. Hydrol. 326, 311–324.

Batelaan, O., De Smedt, F., 2001. WetSpass: a flexible, GIS based, distributed recharge methodology for regional groundwater modelling. IAHS Publ. 11–18.

Bonsor, H.C., MacDonald, A.M., Ahmed, K.M., Burgess, W.G., Basharat, M., Calow, R.C., et al., 2017. Hydrogeological typologies of the Indo-Gangetic basin alluvial aquifer, South AsiaTypologies. Hydrogeol. J. 1–30.

Bredehoeft, J., 2005. The conceptualization model problem—surprise. Hydrogeol. J. 13, 37–46.

Brouyère, S., Carabin, G., Dassargues, A., 2004. Climate change impacts on groundwater resources: modelled deficits in a chalky aquifer, Geer basin, Belgium. Hydrogeol. J. 12, 123–134.

Chakravarti, I.M., Laha, R.G., 1967. Handbook of methods of applied statistics, in: Handbook of Methods of Applied Statistics. John Wiley & Sons.

Chen, Z., Grasby, S.E., Osadetz, K.G., 2004. Relation between climate variability and groundwater levels in the upper carbonate aquifer, southern Manitoba, Canada. J. Hydrol. 290, 43–62.

Chiang, W.-H., Kinzelbach, W., 1998. Processing MODFLOW: a simulation system for modeling groundwater flow and pollution. Softw. Instr. Book Hambg.-Zurich.

Dams, J., Salvadore, E., Van Daele, T., Ntegeka, V., Willems, P., Batelaan, O., 2012. Spatio-temporal impact of climate change on the groundwater system. Hydrol. Earth Syst. Sci. 16, 1517.

Deser, C., Phillips, A., Bourdette, V., Teng, H., 2012. Uncertainty in climate change projections: the role of internal variability. Clim. Dyn. 38, 527–546.

Doherty, J., 1994. PEST: a unique computer program for model-independent parameter optimisation. Water 94 GroundwaterSurface Hydrol. Common Interest Pap. Prepr. Pap. 551.

Döll, P., Hoffmann-Dobrev, H., Portmann, F.T., Siebert, S., Eicker, A., Rodell, M., Strassberg, G., Scanlon, B.R., 2012. Impact of water withdrawals from groundwater and surface water on continental water storage variations. J. Geodyn. 59, 143–156.

Domenico, P.A., Mifflin, M.D., 1965. Water from low-permeability sediments and land subsidence. Water Resour. Res. 1, 563–576.

Domenico, P.A., Schwartz, F.W., 1998. Physical and chemical hydrogeology. Wiley New York.

Draper, D., 1994. Assessment and propagation of model uncertainty. J. R. Stat. Soc. Ser. B 56.

Faisal, I.M., Parveen, S., Kabir, M.R., 2005. Sustainable development through groundwater management: a case study on the Barind tract. Int. J. Water Resour. Dev. 21, 425–435.

Fetter, C.W., 2001. Applied Hydrogeology. 4th Edition, Prentice Hall, Upper Saddle River, 2, 8.

Flato, G., Marotzke, J., Abiodun, B., Braconnot, P., Chou, S.C., Collins, W.J., Cox, P., Driouech, F., Emori, S., Eyring, V., 2013. Evaluation of Climate Models. In: Climate Change 2013: The Physical Science Basis. Contribution of Working Group I to the Fifth Assessment Report of the Intergovernmental Panel on Climate Change. Clim. Change 2013 5, 741–866.

Gaganis, P., Smith, L., 2006. Evaluation of the uncertainty of groundwater model predictions associated with conceptual errors: A per-datum approach to model calibration. Adv. Water Resour. 29, 503–514.

Goderniaux, P., Brouyere, S., Blenkinsop, S., Burton, A., Fowler, H.J., Orban, P., Dassargues, A., 2011. Modeling climate change impacts on groundwater resources using transient stochastic climatic scenarios. Water Resour. Res. 47.

Goderniaux, P., Brouyère, S., Fowler, H.J., Blenkinsop, S., Therrien, R., Orban, P., Dassargues, A., 2009. Large scale surface–subsurface hydrological model to assess climate change impacts on groundwater reserves. J. Hydrol. 373, 122–138.

Goderniaux, P., Brouyère, S., Wildemeersch, S., Therrien, R., Dassargues, A., 2015. Uncertainty of climate change impact on groundwater reserves–application to a chalk aquifer. J. Hydrol. 528, 108–121.

879 Gosling, S., Taylor, R.G., Arnell, N., Todd, M.C., 2011. A comparative analysis of projected impacts of climate
880 change on river runoff from global and catchment-scale hydrological models. Hydrol. Earth Syst. Sci.
881 15, 279–294.
882 Gupta, H. V., Sorooshian, S., & Yapo, P. O. (1999). Status of automatic calibration for hydrologic models:
883 Comparison with multilevel expert calibration. Journal of Hydrologic Engineering, 4(2), 135-143.
884 Hamed, K.H., Rao, A.R., 1998. A modified Mann-Kendall trend test for autocorrelated data. J. Hydrol. 204,
885 182–196.
886 Harbaugh, A.W., McDonald, M.G., 1996. Programmer's documentation for MODFLOW-96, an update to the
887 US Geological Survey modular finite-difference ground-water flow model. US Geological Survey;
888 Branch of Information Services [distributor],.
889 Hassan, A.E., 2004a. A methodology for validating numerical ground water models. Groundwater 42, 347–362.
890 Hassan, A.E., 2004b. Validation of numerical ground water models used to guide decision making. Groundwater
891 42, 277–290.
892 Hawkins, E., Sutton, R., 2012. Time of emergence of climate signals. Geophys. Res. Lett. 39.
893 Hawkins, E., Sutton, R., 2009. The potential to narrow uncertainty in regional climate predictions. Bull. Am.
894 Meteorol. Soc. 90, 1095–1107.
895 Hoeting, J.A., Madigan, D., Raftery, A.E., Volinsky, C.T., 1999. Bayesian model averaging: a tutorial. Stat. Sci.
896 382–401.
897 Højberg, A.L., Refsgaard, J.C., 2005. Model uncertainty–parameter uncertainty versus conceptual models. Water
898 Sci. Technol. 52, 177–186.
899 Holman, I.P., Allen, D.M., Cuthbert, M.O., Goderniaux, P., 2012. Towards best practice for assessing the
900 impacts of climate change on groundwater. Hydrogeol. J. 20, 1–4.
901 Hunter, J.D., 2007. Matplotlib: A 2D graphics environment. Comput. Sci. Eng. 9, 90–95.
902 IPCC, 2013. Summary for Policymakers. In: Climate Change 2013: The Physical Science Basis. Contribution of
903 Working Group I to the Fifth Assessment Report of the Intergovernmental Panel on Climate Change
904 [Stocker, T.F., D. Qin, G.-K. Plattner, M. Tignor, S.K. Allen, J. Boschung, A. Nauels, Y. Xia, V. Bex
905 and P.M. Midgley (eds.)]. Cambridge University Press, Cambridge, United Kingdom and New York,
906 NY, USA.
907 Jackson, C.R., Meister, R., Prudhomme, C., 2011. Modelling the effects of climate change and its uncertainty on
908 UK Chalk groundwater resources from an ensemble of global climate model projections. J. Hydrol.
909 399, 12–28.

Jahan, C.S., Mazumder, Q.H., Ghose, S.K., Asaduzzaman, M., 1994. Specific yield evaluation: Barind area, Bangaladesh. Geol. Soc. India 44(3), 283–290.

Jahani, C.S., Ahmed, M., 1997. Flow of groundwater in the Barind area, Bangladesh: implication of structural framework. Geol. Soc. India 50, 743–752.

Johnson, A.I., 1967. Specific yield: compilation of specific yields for various materials. US Government Printing Office.

Karim, Z., 1997. Accelerated agricultural growth in Bangladesh, in: Seminar on Agricultural Research on Development in Bangladesh. BARC, Dhaka, Bangladesh.

Li, X., Tsai, F.T.-C., 2009. Bayesian model averaging for groundwater head prediction and uncertainty analysis using multimodel and multimethod. Water Resour. Res. 45.

McDonald, M.G., Harbaugh, A.W., 1988. A modular three-dimensional finite-difference ground-water flow model.

McKinney, W., 2010. Data structures for statistical computing in python, in: Proceedings of the 9th Python in Science Conference. SciPy Austin, TX, pp. 51–56.

Mehl, S., Hill, M. C., 2010. Grid-size dependence of Cauchy boundary conditions used to simulate stream–aquifer interactions. Adv Water Resour., 33(4), 430-442.

Michael, H.A., Voss, C.I., 2009a. Estimation of regional-scale groundwater flow properties in the Bengal Basin of India and Bangladesh. Hydrogeol. J. 17, 1329–1346.

Michael, H.A., Voss, C.I., 2009b. Controls on groundwater flow in the Bengal Basin of India and Bangladesh: regional modeling analysis. Hydrogeol. J. 17, 1561.

Mondal, M.H., 2010. Crop agriculture of Bangladesh: Challenges and opportunities. Bangladesh J. Agric. Res. 35, 235–245.

Mondal, M.H., 2005. Challenges and Opportunities of sustainable crop production in Bangladesh, in: Eighth Biennial Agronomy Convention. Bangladesh Society of Agronomy.

Moriasi, D.N., Arnold, J.G., Van Liew, M.W., Bingner, R.L., Harmel, R.D., Veith, T.L., 2007. Model evaluation guidelines for systematic quantification of accuracy in watershed simulations. Trans. ASABE 50, 885–900.

Mustafa, S.M.T., Abdollahi, K., Verbeiren, B., Huysmans, M., 2017a. Identification of the influencing factors on groundwater drought and depletion in northwestern Bangladesh. Hydrogeol. J. 1–19.

939 Mustafa, S.M.T., Vanuytrecht, E., Huysmans, M., 2017b. Combined deficit irrigation and soil fertility
940 management on different soil textures to improve wheat yield in drought-prone Bangladesh. Agric.
941 Water Manag. 191, 124–137.
942 Mustafa, S.M.T., Nossent, J., Ghysels, G., Huysmans, M., 2018. Estimation and impact assessment of input and
943 parameter uncertainty in predicting groundwater flow with a fully distributed model. Water Resour.
944 Res. 54(9), 6585-6608.
945 Nakicenovic, N., Alcamo, J., Grubler, A., Riahi, K., Roehrl, R.A., Rogner, H.-H., Victor, N., 2000. Special
946 Report on Emissions Scenarios (SRES), A Special Report of Working Group III of the
947 Intergovernmental Panel on Climate Change. Cambridge University Press.
948 Neukum, C., Azzam, R., 2012. Impact of climate change on groundwater recharge in a small catchment in the
949 Black Forest, Germany. Hydrogeol. J. 20, 547–560.
950 Neuman, S.P., 2003. Maximum likelihood Bayesian averaging of uncertain model predictions. Stoch. Environ.
951 Res. Risk Assess. 17, 291–305.
952 Ntegeka, V., Baguis, P., Roulin, E., Willems, P., 2014. Developing tailored climate change scenarios for
953 hydrological impact assessments. J. Hydrol. 508, 307–321.
954 Poeter, E., Anderson, D., 2005. Multimodel ranking and inference in ground water modeling. Groundwater 43,
955 597–605.
956 Qureshi, A.S., Ahmed, Z., Krupnik, T.J., 2014. Groundwater management in Bangladesh: an analysis of
957 problems and opportunities.
958 Rahman, M.M., Kamal, A.H.M., Al Mamun, A., Miah, M.S.U., 2011. Study on the irrigation water distribution
959 system developed by barind multipurpose development authority. J. Bangladesh Assoc. Young Res. 1,
960 63–71.
961 Rahman, M.M., Shahid, S., 2004. Modeling groundwater flow for the delineation of wellhead protection area
962 around a water-well at Nachole of Bangladesh. J. Spat. Hydrol. 4.
963 Rahman, M.R., Bulbul, S.H., 2015. Adoption of water saving irrigation techniques for sustainable rice
964 production in Bangladesh. Environ. Ecol. Res. 3, 1–8.
965 Refsgaard, J.C., Van der Sluijs, J.P., Brown, J., Van der Keur, P., 2006. A framework for dealing with
966 uncertainty due to model structure error. Adv. Water Resour. 29, 1586–1597.
967 Rodell, M., Velicogna, I., Famiglietti, J.S., 2009. Satellite-based estimates of groundwater depletion in India.
968 Nature 460, 999–1002.

969 Rojas, R., Feyen, L., Dassargues, A., 2008. Conceptual model uncertainty in groundwater modeling: Combining
970 generalized likelihood uncertainty estimation and Bayesian model averaging. Water Resour. Res. 44.
971 Rojas, R., Kahunde, S., Peeters, L., Batelaan, O., Feyen, L., Dassargues, A., 2010. Application of a multimodel
972 approach to account for conceptual model and scenario uncertainties in groundwater modelling. J.
973 Hydrol. 394, 416–435.
974 Scanlon, B.R., Faunt, C.C., Longuevergne, L., Reedy, R.C., Alley, W.M., McGuire, V.L., McMahon, P.B., 2012.
975 Groundwater depletion and sustainability of irrigation in the US High Plains and Central Valley. Proc.
976 Natl. Acad. Sci. 109, 9320–9325.
977 Scibek, J., Allen, D.M., Cannon, A.J., Whitfield, P.H., 2007. Groundwater–surface water interaction under
978 scenarios of climate change using a high-resolution transient groundwater model. J. Hydrol. 333, 165–
979 181.
980 Sen, P.K., 1968. Estimates of the regression coefficient based on Kendall's tau. J. Am. Stat. Assoc. 63, 1379–
981 1389.
982 Shahid, S., 2011. Impact of climate change on irrigation water demand of dry season Boro rice in northwest
983 Bangladesh. Clim. Change 105, 433–453.
984 Shahid, S., 2009. Spatial assessment of groundwater demand in Northwest Bangladesh. Int. J. Water 5, 267–283.
985 Shahid, S., Behrawan, H., 2008. Drought risk assessment in the western part of Bangladesh. Nat. Hazards 46,
986 391–413.
987 Shamsudduha, M., Chandler, R.E., Taylor, R.G., Ahmed, K.M., 2009. Recent trends in groundwater levels in a
988 highly seasonal hydrological system: the Ganges-Brahmaputra-Meghna Delta. Hydrol. Earth Syst. Sci.
989 13, 2373–2385.
990 Shamsudduha, M., Taylor, R.G., Ahmed, K.M., Zahid, A., 2011. The impact of intensive groundwater
991 abstraction on recharge to a shallow regional aquifer system: evidence from Bangladesh. Hydrogeol. J.
992 19, 901–916.
993 Shamsudduha, M., Taylor, R.G., Chandler, R.E., 2015. A generalized regression model of arsenic variations in
994 the shallow groundwater of Bangladesh. Water Resour. Res. 51, 685–703.
995 Stoll, S., Franssen, H.H., Butts, M., Kinzelbach, W., 2011. Analysis of the impact of climate change on
996 groundwater related hydrological fluxes: a multi-model approach including different downscaling
997 methods. Hydrol. Earth Syst. Sci. 15, 21.

998 Sulis, M., Paniconi, C., Marrocu, M., Huard, D., Chaumont, D., 2012. Hydrologic response to multimodel
999 climate output using a physically based model of groundwater/surface water interactions. Water Resour.
1000 Res. 48.
1001 Taylor, K.E., Stouffer, R.J., Meehl, G.A., 2012. An overview of CMIP5 and the experiment design. Bull. Am.
1002 Meteorol. Soc. 93, 485–498.
1003 Taylor, R.G., Scanlon, B., Döll, P., Rodell, M., Van Beek, R., Wada, Y., Longuevergne, L., Leblanc, M.,
1004 Famiglietti, J.S., Edmunds, M., 2013. Ground water and climate change. Nat. Clim. Change 3, 322–329.
1005 Tebaldi, C., Knutti, R., 2007. The use of the multi-model ensemble in probabilistic climate projections. Philos.
1006 Trans. R. Soc. Lond. Math. Phys. Eng. Sci. 365, 2053–2075.
1007 Teklesadik, A.D., Alemayehu, T., van Griensven, A., Kumar, R., Liersch, S., Eisner, S., Tecklenburg, J.,
1008 Ewunte, S., Wang, X., 2017. Inter-model comparison of hydrological impacts of climate change on the
1009 Upper Blue Nile basin using ensemble of hydrological models and global climate models. Clim.
1010 Change 141, 517–532.
1011 Troldborg, L., Refsgaard, J.C., Jensen, K.H., Engesgaard, P., 2007. The importance of alternative conceptual
1012 models for simulation of concentrations in a multi-aquifer system. Hydrogeol. J. 15, 843–860.
1013 van Roosmalen, L., Sonnenborg, T.O., Jensen, K.H., 2009. Impact of climate and land use change on the
1014 hydrology of a large-scale agricultural catchment. Water Resour. Res. 45.
1015 Van Straten, G.T., Keesman, K.J., 1991. Uncertainty propagation and speculation in projective forecasts of
1016 environmental change: A lake-eutrophication example. J. Forecast. 10, 163–190.
1017 Van Vuuren, D.P., Edmonds, J., Kainuma, M., Riahi, K., Thomson, A., Hibbard, K., Hurtt, G.C., Kram, T.,
1018 Krey, V., Lamarque, J.-F., 2011. The representative concentration pathways: an overview. Clim.
1019 Change 109, 5.
1020 Vrugt, J.A., 2016. MODELAVG: A MATLAB Toolbox for Postprocessing of Model Ensembles. Department of
1021 Civil and Environmental Engineering, University of California Irvine, 4130 Engineering Gateway,
1022 Irvine, CA.
1023 Wada, Y., Van Beek, L.P., Wanders, N., Bierkens, M.F., 2013. Human water consumption intensifies
1024 hydrological drought worldwide. Environ. Res. Lett. 8, 34036.
1025 Wada, Y., Wisser, D., Bierkens, M.F.P., 2014. Global modeling of withdrawal, allocation and consumptive use
1026 of surface water and groundwater resources. Earth Syst. Dyn. 5, 15.

1027 Walt, S. van der, Colbert, S.C., Varoquaux, G., 2011. The NumPy array: a structure for efficient numerical
1028 computation. Comput. Sci. Eng. 13, 22–30.
1029 Willems, P., 2012. Model uncertainty analysis by variance decomposition. Phys. Chem. Earth Parts ABC 42,
1030 21–30.
1031 Wisser, D., Frolking, S., Douglas, E.M., Fekete, B.M., Vörösmarty, C.J., Schumann, A.H., 2008. Global
1032 irrigation water demand: Variability and uncertainties arising from agricultural and climate data sets.
1033 Geophys. Res. Lett. 35.
1034 Woldeamlak, S.T., Batelaan, O., De Smedt, F., 2007. Effects of climate change on the groundwater system in the
1035 Grote-Nete catchment, Belgium. Hydrogeol. J. 15, 891–901.
1036 Wu, J., Zeng, X., 2013. Review of the uncertainty analysis of groundwater numerical simulation. Chin. Sci. Bull.
1037 58, 3044–3052.
1038 Ye, M., Neuman, S.P., Meyer, P.D., 2004. Maximum likelihood Bayesian averaging of spatial variability models
1039 in unsaturated fractured tuff. Water Resour. Res. 40.
1040 Zhou, Y., Herath, H., 2017. Evaluation of alternative conceptual models for groundwater modelling. Geosci.
1041 Front. 8, 437–443.
1042
1043